



Published in final edited form as:

Cell Rep. 2022 September 06; 40(10): 111312. doi:10.1016/j.celrep.2022.111312.

Molecular convergence between Down syndrome and fragile X syndrome identified using human pluripotent stem cell models

Sara G. Susco^{1,2}, Sulagna Ghosh¹, Patrizia Mazzucato¹, Gabriella Angelini¹, Amanda Beccard¹, Victor Barrera³, Martin H. Berryer^{1,2}, Angelica Messana¹, Daisy Lam¹, Dane Z. Hazelbaker¹, Lindy E. Barrett^{1,2,4,*}

¹Stanley Center for Psychiatric Research, Broad Institute of MIT and Harvard, Cambridge, MA 02142, USA

²Department of Stem Cell and Regenerative Biology, Harvard University, Cambridge, MA 02138, USA

³Bioinformatics Core, Department of Biostatistics, Harvard T.H. Chan School of Public Health, Boston, MA 02115, USA

⁴Lead contact

SUMMARY

Down syndrome (DS), driven by an extra copy of chromosome 21 (HSA21), and fragile X syndrome (FXS), driven by loss of the RNA-binding protein FMRP, are two common genetic causes of intellectual disability and autism. Based upon the number of DS-implicated transcripts bound by FMRP, we hypothesize that DS and FXS may share underlying mechanisms. Comparing DS and FXS human pluripotent stem cell (hPSC) and glutamatergic neuron models, we identify increased protein expression of select targets and overlapping transcriptional perturbations. Moreover, acute upregulation of endogenous FMRP in DS patient cells using CRISPRa is sufficient to significantly reduce expression levels of candidate proteins and reverse 40% of global transcriptional perturbations. These results pinpoint specific molecular perturbations shared between DS and FXS that can be leveraged as a strategy for target prioritization; they also provide evidence for the functional relevance of previous associations between FMRP targets and disease-implicated genes.

Graphical Abstract

This is an open access article under the CC BY-NC-ND license (<http://creativecommons.org/licenses/by-nc-nd/4.0/>).

*Correspondence: lbarrett@broadinstitute.org.

AUTHOR CONTRIBUTIONS

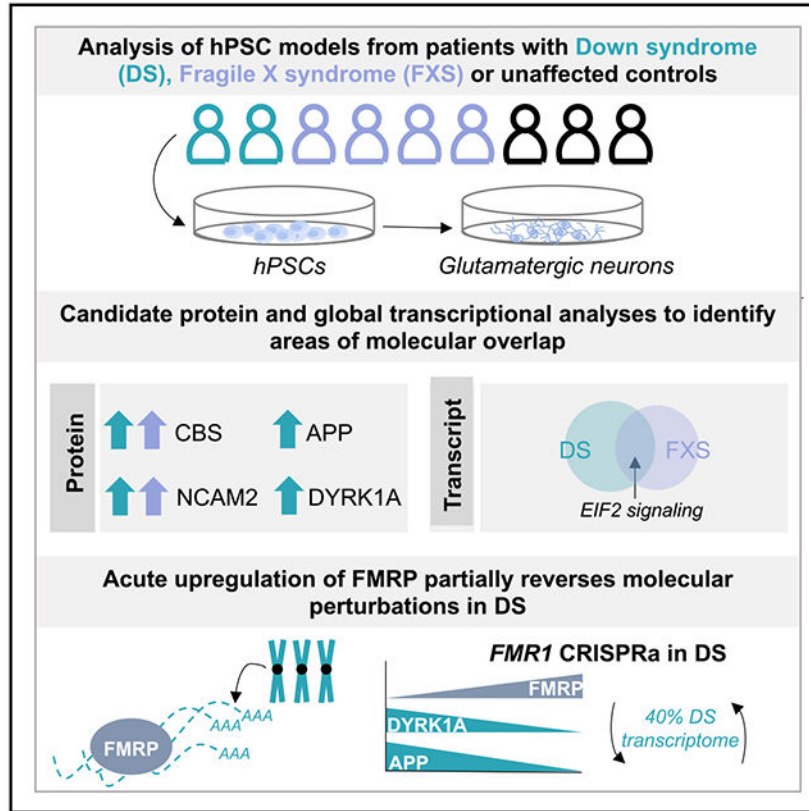
L.E.B. and S.G.S. conceived the project and wrote the manuscript. S.G.S. performed stem cell and neuron culture, RNA-seq, western blot, and analyses. P.M., G.A., A.B., A.M., D.Z.H., and D.L. generated edited cell lines and reagents and provided technical support for CRISPRa experiments. V.B. performed FXS and DS RNA-seq analyses. M.H.B. assisted with CRISPRa RNA-seq experiments. S.G. provided analytical support and L.E.B. supervised the study and secured funding. All authors discussed results and edited the manuscript.

SUPPLEMENTAL INFORMATION

Supplemental information can be found online at <https://doi.org/10.1016/j.celrep.2022.111312>.

DECLARATION OF INTERESTS

The authors declare no competing interests.



In brief

Many neurodevelopmental disorders driven by distinct genetic alterations share phenotypes, but the extent to which they share underlying mechanisms remains an important unanswered question. Using transcript and protein-level analyses in human cellular models, Susco et al. uncover specific areas of molecular convergence between Down syndrome and fragile X syndrome.

INTRODUCTION

Down syndrome (DS) is the most common genetic cause of intellectual disability with a frequency of approximately 1 in 700 live births, driven by triplication of the smallest human autosome (HSA21). Although DS is caused by a defined chromosomal change with a predicted directionality of effect, molecular mechanisms and pharmacological interventions remain elusive. This is in part due to the large number of genes dysregulated by HSA21 triplication, directly or indirectly. Studies across diverse organisms generally support the notions that: (1) many but not all genes encoded on HSA21 show the expected pattern of upregulation in DS compared with euploid controls; (2) a majority of all differentially expressed genes (DEGs) in a given system are not encoded on HSA21; and (3) there is high inter-individual variation in gene expression changes (Hibaoui et al., 2014; Lockstone et al., 2007; Prandini et al., 2007). Thus, target prioritization in DS remains an enormous challenge.

Interestingly, DS shares some patient and cellular phenotypes with fragile X syndrome (FXS), the most common inherited cause of intellectual disability and leading monogenic cause of autism, affecting approximately 1 in 4,000 males and 1 in 8,000 females. In most cases FXS is driven by a tri-nucleotide repeat expansion in the 5' UTR of the *fragile X messenger ribonucleoprotein 1 (FMR1)* gene, which leads to epigenetic silencing and complete loss of the encoded RNA binding protein FMRP (Bagni et al., 2012; Darnell et al., 2011; Dichtenberg et al., 2008). While both DS and FXS are characterized by broad phenotypic variability, patients with DS and FXS share intellectual disability and deficits in expressive communication, as well as increased rates of autism, seizure disorders, and mental health disorders compared with the general population (Capone et al., 2006; Del Hoyo Soriano et al., 2020; Finestack et al., 2009; Jensen and Bulova, 2014; Martin et al., 2009; Tranfaglia, 2012). Other phenotypes diverge; unlike patients with FXS, patients with DS are at increased risk for childhood leukemias and DS is one of the most common genetic causes of early-onset Alzheimer's disease (Mateos et al., 2015; Tcw and Goate, 2017). At the cellular level, both DS and FXS have been associated with alterations in dendritic spine morphology, decreased synaptic plasticity, and neurogenesis (Faundez et al., 2018; Haas et al., 2013; Martinez-Cerdeno, 2017), as well as mitochondrial and metabolic dysfunction (D'Antoni et al., 2020; Panagaki et al., 2019; Weisz et al., 2018). Moreover, previous studies have analyzed FMRP targets from mouse brain against genes dysregulated in DS, identifying general enrichment as well as increased protein-protein interaction networks (De Toma et al., 2016; Faundez et al., 2018).

Notably, multiple studies also report gene set overlap between FMRP targets and genes implicated in autism, schizophrenia, and bipolar disorder (Clifton et al., 2020; Darnell et al., 2011; Iossifov et al., 2014; Sanders et al., 2015; Schizophrenia Working Group of the Psychiatric Genomics Consortium, 2014). For example, a recent study using multiple mouse and human FMRP target datasets found significant enrichment among high-confidence FMRP targets for common and rare variants associated with schizophrenia (Clifton et al., 2020). In general, such an overlap is suggestive of convergent molecular mechanisms and could be leveraged to identify high-priority gene targets for functional investigation. However, the hypothesis that gene set overlap leads to dysregulation of specific shared molecules or pathways has not been assessed experimentally. Moreover, while neurodevelopmental disorders may have overlapping phenotypes, the extent to which those shared phenotypes are driven by dysregulation of distinct versus overlapping genes and pathways remains to be determined.

Here, we sought to investigate two primary hypotheses. First, does overlap between FMRP targets and genes implicated in DS lead to shared molecular perturbations in FXS and DS? Second, is there a causal relationship between FMRP and DS-implicated genes? DS is well suited for these analyses as most patients harbor an identical, defined chromosomal abnormality (i.e., triplication of HSA21). In the cases of autism, schizophrenia, and bipolar disorder, different patients frequently harbor different sets of known risk variants in addition to unmapped disease risk. Leveraging human pluripotent stem cell (hPSC) models of both DS and FXS, we identified increased protein expression of select FMRP targets encoded on HSA21 and implicated in DS, as well as a set of overlapping transcriptional perturbations. Notably, acute upregulation of endogenous FMRP through CRISPR activation (CRISPRa)

in DS patient cells was sufficient to significantly reduce protein expression levels of select FMRP targets implicated in DS and drove a sustained reversal in over 40% of the global transcriptional perturbations in DS. These analyses identify specific points of molecular connectivity between DS and FXS using physiological relevant human cellular models, which can be used to prioritize genes and pathways for further interrogation; they also provide evidence for the functional relevance of previous gene set associations between FMRP targets and disease-implicated genes.

RESULTS

DS and FXS share specific protein-level perturbations in hPSC models

To test the hypothesis that overlap between FMRP targets and DS-implicated genes leads to dysregulation of shared molecules in DS and FXS, we first took a candidate approach. Both DS and FXS are canonically associated with increased protein expression through either increased gene dosage (DS) or loss of translational repression (FXS), leading to the prediction that FMRP targets implicated in DS would be increased in both diseases. However, effect sizes are reportedly modest in both diseases and protein-level changes in FXS have been confirmed for only a small number of FMRP targets (Davis and Broadie, 2017). We first expanded previous comparisons of DS-implicated genes and FMRP targets from mouse brain (De Toma et al., 2016; Faundez et al., 2018) to include a recently published FMRP target dataset from human brain (Tran et al., 2019) and human cellular models (Kang et al., 2021). Of the 235 protein coding genes reportedly encoded on HSA21 by Ensembl, 28.9% or 68 genes have been identified as direct FMRP targets in these systems (Table S1). From this analysis, we selected a set of: (1) protein coding FMRP targets identified from a minimum of two independent human FMRP target datasets and encoded on HSA21, (2) targets reported to be upregulated in DS at the protein level in model systems or post-mortem tissue, and (3) targets reported to play a role in DS disease biology in animal or cellular models. Specifically, we selected cystathionine beta-synthase (CBS) (enzyme in the transsulfuration pathway), neuronal cell adhesion molecule 2 (NCAM2) (cell adhesion molecule), amyloid beta precursor protein (APP) (cell surface receptor), and dual specificity tyrosine phosphorylation regulated kinase 1A (DYRK1A) (tyrosine kinase).

Based on data from large-scale hPSC studies indicating that increasing the number of independent genetic backgrounds adds more value than clonal replicates from a smaller set of backgrounds (Germain and Testa, 2017; Hoffman et al., 2019; Rouhani et al., 2014), combined with the significant heterogeneity reported among patients with DS and FXS (Deutsch et al., 2005; Jacquemont et al., 2018; Prandini et al., 2007), we employed a combination of both independent hPSC lines as well as isogenic comparisons. Specifically, we utilized an isogenic pair of euploid control and DS patient-induced iPSC lines generated from mosaic patient fibroblasts (DS2U and DS1, respectively) (Weick et al., 2013), an additional non-isogenic DS patient iPSC line (2DS3) (Weick et al., 2013), and an additional non-isogenic control iPSC line (CW60278; CIRM/FujiFilm CDI). We also reprogrammed three iPSC lines from XY FXS patient fibroblasts obtained from Coriell (FXS iPSC A, FXS iPSC B, FXS iPSC C), in addition to our previously generated isogenic *FMR1*^{+/+} and *FMR1*^{-/-} CRISPR engineered lines (Susco et al., 2020), confirming

appropriate karyotypes, genotypes, and pluripotency (Figures 1A and 1B; Table S2 and data not shown). As *FMR1* is located on the X chromosome, our XY *FMR1*-deficient cell line is denoted as *FMR1*^{Y/-} and the isogenic control as *FMR1*^{Y/+}. In total, this allowed us to analyze three control cell lines, four FXS cell lines, and two DS cell lines per target, including an isogenic pair within each control-disease state comparison. We also generated glutamatergic neurons from these cell lines through developmental patterning and ectopic *Neurogenin2* (*Ngn2*) expression; neurons most closely resemble fetal brain cells from upper cortical layers and we and others have performed extensive characterization of these cellular substrates at molecular and physiological levels (Chanda et al., 2019; Lin et al., 2018; Nehme et al., 2018; Pak et al., 2015; Susco et al., 2020; Yi et al., 2016; Zhang et al., 2013).

Notably, CBS protein expression levels were significantly upregulated in both FXS ($p = 0.0251$) and DS ($p = 0.0213$) hPSC lines compared with controls, with similar magnitudes of effect (Figures 1C and S1). While NCAM2 protein expression levels were significantly upregulated across DS ($p = 0.0180$) but not FXS ($p = 0.1597$) hPSC lines using grouped analyses, we noted large inter-individual variation for this target (Figures 1D and S1). We therefore extracted the isogenic *FMR1*^{Y/+} and *FMR1*^{Y/-} comparison, which revealed significant NCAM2 protein upregulation following FMRP loss in an isogenic setting ($p = 0.0024$); this was also the case for many of the individual non-isogenic disease-control comparisons (Figures 1E and S1). Here, the signal in the grouped analysis was likely obscured by the broad distribution of NCAM2 protein expression levels observed across different individuals, making the isogenic comparison particularly valuable. Importantly, both CBS and NCAM2 have reported roles in DS disease biology of relevance to FXS (Marechal et al., 2019; Mouton-Liger et al., 2011; Raveau et al., 2017; Sheng et al., 2018). Overexpression of CBS has been associated with mitochondrial dysfunction in DS (Panagaki et al., 2019; Szabo, 2020) and is reportedly necessary and sufficient for induction of a subset of cognitive phenotypes in mouse models (Marechal et al., 2019), with mitochondrial and cognitive dysfunction also observed in FXS (D'Antoni et al., 2020; Weisz et al., 2018). Overexpression of NCAM2 reportedly inhibits maturation of dendritic spines and synapses in DS mouse models (Sheng et al., 2018), with reduced maturation of dendritic spines and synapses also observed in FXS (Martinez-Cerdeno, 2017). *NCAM2* has also previously been implicated in developmental delay (Petit et al., 2015) as well as synaptic dysfunction in Alzheimer's disease (Han et al., 2010; Kimura et al., 2007; Leshchyns'ka et al., 2015), which may point to broader roles in developmental or degenerative disease processes.

APP ($p = 0.0012$) and DYRK1A ($p < 0.0001$) were significantly upregulated at the protein level in DS patient cell lines compared with controls but did not show evidence for protein-level changes across FXS cell lines (Figures 1F–1G and S1). Of note, several studies report upregulated APP protein expression in FXS mouse models (Khalfallah et al., 2017; Westmark et al., 2011, 2016); however, our data do not support broad upregulation of APP across FXS hPSCs (Figures 1F and S1). As expected, protein-level effect sizes were modest in both diseases.

These data confirm that overlap between FMRP targets and DS-implicated genes can translate into shared protein-level perturbations in FXS and DS, and further identify *CBS* and *NCAM2* as priority genes for further interrogation in FXS based on the relevance

of their known biological roles in DS. These analyses also underscore that gene set overlap does not necessarily result in coordinate protein-level changes, which is an important consideration when interpreting overlap analyses of FMRP targets and other neurodevelopmental disorders.

Mapping global transcriptional dysregulation in DS and FXS hPSC models

In addition to candidate protein-level analyses, we next took an unbiased approach and assessed global transcriptional dysregulation. To eliminate variability due to genetic background differences within disease-control comparisons, we performed RNA-seq analyses using isogenic DS and euploid cell lines (Weick et al., 2013) as well as isogenic *FMR1*^{+/+} and *FMR1*^{-/-} cell lines (Susco et al., 2020), analyzing both hPSCs as well as glutamatergic neurons. To minimize batch effects, all DS and FXS samples were processed as part of the same sequencing experiment, with five replicates per genotype and cell type and an adjusted p value cutoff of 0.05 (Figures 2A–2M; Tables S3 and S4). Thus, we were able to directly compare DS and FXS transcriptomes in the same cell types in a batch-controlled setting. Starting with the DS RNA-seq dataset, we observed broad transcriptional dysregulation in both hPSCs and neurons, with roughly equal numbers of significantly DEGs upregulated and downregulated in each cell type (Figures 2B and 2C; Table S3). Most HSA21-encoded genes were upregulated in DS cells compared with euploid controls around the expected +0.58 log₂ fold change, including canonical DS-implicated genes, such as *DYRK1A* and *APP* (Figures 2D and 2E; Table S3). Magnitudes of effect across the entire dataset ranged from an average log₂ fold change of –0.70 and +0.76 in hPSCs and –0.84 and +1.53 in neurons (Table S3). The most significantly DEGs in our DS datasets were not genes encoded on HSA21. The mitochondrial and transcriptional regulator *coiled-coil-helix-coiled-coil-helix domain containing 2* (*CHCHD2*), which is a key mediator of the oxidative phosphorylation process (Kee et al., 2021) and is encoded on chromosome 7, was the most significant DEG in our DS hPSC dataset, while the proteolipid *neuronatin* (*NNAT*) implicated in synaptic plasticity (Joseph, 2014) and encoded on chromosome 20, was the most significant DEG in our DS neuron dataset (Figure 2F; Table S3). These examples highlight the striking indirect effects of HSA21 triplication, and the challenge in identifying all potentially relevant gene perturbations. Using Ingenuity Pathway Analysis (IPA), we identified the top 5 most significant canonical pathways disrupted in DS hPSCs and neurons; terms such as “EIF2 signaling” were present in both cell types, while others such as “actin cytoskeleton signaling” were only found in hPSCs, and “axonal guidance signaling” only in neurons (Figures 2G and 2H).

In our FXS RNA-seq datasets, we observed fewer dysregulated genes compared with our DS datasets, but again roughly equal numbers of upregulated and downregulated DEGs in each cell type (Figures 2J and 2K; Table S4). The number of DEGs in neurons was particularly low, suggestive of modest transcriptional dysregulation in this cell type or developmental stage (Figure 2K). Overall, magnitudes of effect in FXS were modest, with an average log₂ fold change of –0.44 and +0.66 in hPSCs and –1.22 and +1.66 in neurons (Table S4). These results are generally consistent with diverse functions of FMRP in RNA processing, including translational regulation, splicing, editing, and trafficking, in addition to impacts on transcript abundance (Alpatov et al., 2014; Chakraborty et al., 2020; Chen et al., 2014;

D'Souza et al., 2018; Darnell et al., 2011; Dichtenberg et al., 2008; Didiot et al., 2008; Edens et al., 2019; Kim et al., 2009; Kim et al., 2019; Tran et al., 2019; Tsang et al., 2019; Zhou et al., 2017). Taking the top 5 most significant canonical pathways disrupted in FXS hPSCs revealed terms, such as “EIF2 signaling,” “mTOR signaling,” and “PI3K/AKT signaling,” all of which have previously been associated with FXS (Hoeffler et al., 2012; Raj et al., 2021; Utami et al., 2020) (Figure 2L). Given the small nature of the FXS neuronal dataset, few pathways were identified (Figure 2M). Of note, EIF2 signaling was a top dysregulated pathway in both the DS and FXS datasets, suggesting that both diseases may converge on translation in human cellular models. Indeed, translation is widely reported to be disrupted in FXS (Darnell et al., 2011; Greenblatt and Spradling, 2018); while less is known about translational regulation in DS, a recent study identified translational abnormalities in both mouse and human DS models (Zhu et al., 2019).

Collectively, our batch-controlled global transcriptional analyses of DS and FXS human cellular models reveal broad transcriptional re-wiring in DS, more modest transcriptional changes in FXS, and identify EIF2 signaling as a shared pathway disruption.

Transcriptional overlap between DS and FXS hPSC models

We next cross-referenced the DEGs from our established DS and FXS global transcriptional datasets, which revealed significant overlap between dysregulated genes at the hPSC level ($p = 3.19 \times 10^{-33}$); in total 477 DEGs were shared between datasets, representing approximately one-third of all DEGs found in FXS hPSCs (Figure 3A). Differential gene expression patterns in neurons also showed significant overlap ($p = 0.00495$); nearly one-third of DEGs in FXS were shared with DS, although the dataset size disparities clearly illustrate that fewer of the transcriptional changes in DS were also shared with FXS (Figure 3A). *CHCHD2* was the most significant DEG in both the DS hPSC dataset ($p = 4.96 \times 10^{-134}$) and the FXS hPSC dataset ($p = 3.68 \times 10^{-52}$), with dramatic downregulation observed in both disease models (Figures 3B and 2F; Tables S3 and S4). Rare mutations in *CHCHD2* have been associated with several neurodegenerative diseases (Kee et al., 2021) and we noted that *CHCHD2* expression levels continued to be dramatically downregulated in DS neurons, but not in FXS neurons (Tables S3 and S4). Other genes of note that were coordinately dysregulated included the protein glycosylation factor *tumor suppressor candidate 3 (TUSC3)*, the putative magnesium transporter *NIPA magnesium transporter 2 (NIPA2)*, the transcriptional regulator *SRY-box transcription factor 11 (SOX11)*, and the alternative splicing regulator *NOVA alternative splicing regulator 2 (NOVA2)* (Figure 3B; Tables S3 and S4), all of which have been independently implicated in neurodevelopmental disorders (Garshasbi et al., 2008; Mattioli et al., 2020; Tsurusaki et al., 2014; Xie et al., 2014). For example, *TUSC3* was downregulated in both DS and FXS hPSC models, and mutations in this gene have previously been reported to drive nonsyndromic autosomal recessive mental retardation (Garshasbi et al., 2008) while *NOVA2* was coordinately downregulated between DS and FXS neuronal models (Figure 3B), with frameshift mutations in *NOVA2* reported to drive a severe neurodevelopmental disorder (Mattioli et al., 2020).

To understand the degree of overlap in other disease contexts, we also compared our DS and FXS transcriptional datasets with published datasets of genes dysregulated in human cellular models of Alzheimer's disease driven by an *APOE4* variant (Lin et al., 2018) as well as human cellular models of Angelman syndrome driven by loss of *UBE3A* (Sun et al., 2019), generated with the same neuronal differentiation paradigm used in our study. When comparing the Alzheimer's disease dataset with our DS dataset and FXS dataset we identified significant under-enrichment in both cases (Figure S2), consistent with non-overlapping transcriptional changes. For the Angelman syndrome dataset, we observed no significant overlap with the FXS dataset, but we did observe significant overlap with the DS dataset (Figure S2), suggesting that there could be a set of shared gene changes between DS and Angelman syndrome.

Together, these data identify transcriptional overlap between DS and FXS in human cellular models and pinpoint specific genes coordinately dysregulated in both diseases; in some cases, mutations in these genes are also known to drive another neurodevelopmental disorder, strengthening the likelihood that their dysregulation in the context of DS and FXS may play a role in disease biology.

FMRP upregulation is sufficient to reduce expression levels of select DS-implicated proteins

We next sought to establish a causal, or direct molecular relationship, between FMRP and DS-implicated transcript targets using a method orthogonal to IP-based FMRP binding datasets. Specifically, we hypothesized that increasing FMRP dosage in the context of DS could modulate target expression, given that many HSA21-encoded transcripts are upregulated in DS and reportedly bound by FMRP (Table S1); FMRP target modulation could be in the form of transcriptional or translational regulation. CRISPRa technologies, which fuse deactivated Cas9 to transcriptional activation domains, have emerged as a powerful tool for functional genomics, facilitating transient and reversible activation of gene expression. We therefore stably introduced an inducible CRISPRa construct into the AAVS1 safe-harbor locus of the DS patient iPSC line DS1, and delivered a multiplexed piggyBac guide RNA (gRNA) vector containing three *FMR1* activating gRNAs (Hazelbaker et al., 2020) to facilitate acute and transient upregulation of endogenous FMRP (DS-CRISPRa; Figure 4A).

As expected, doxycycline induction of *FMR1* in the DS-CRISPRa cell line led to efficient upregulation of FMRP expression at both the 48 h ($p = 0.0210$) and 120 h ($p = 0.0001$) time points, which returned to baseline after removal of doxycycline (Figure 4B). Importantly, inducing FMRP with CRISPRa had no impact on expression levels of FMRP's autosomal paralog FXR1P, supporting the specificity of our CRISPRa system (Figure 4C). Acute upregulation of endogenous FMRP was sufficient to significantly reduce protein expression levels of DYRK1A in the DS-CRISPRa line after 120 h ($p = 0.0388$) (Figure 4D). Here, transient FMRP upregulation led to a sustained reduction in DYRK1A expression that persisted in the post-treatment condition ($p = 0.0182$) (Figure 4D). DYRK1A is independently implicated in both intellectual disability and autism (Courcet et al., 2012; Deciphering Developmental Disorders, 2017; Duchon and Herault, 2016; Faundez et al.,

2018; O’Roak et al., 2012; Satterstrom et al., 2020), and clinical trials have attempted to normalize *DYRK1A* with the goal of improving cognitive function in patients with DS (de la Torre et al., 2016). FMRP upregulation in the DS-CRISPRa cell line also led to a significant reduction in APP expression levels at 48 h ($p = 0.0387$), which began to recover by 120 h (Figure 4E). *APP* is thought to act as a primary driver allele for AD pathogenesis in DS (Doran et al., 2017; Tcw and Goate, 2017; Teller et al., 1996). By contrast, acute upregulation of FMRP had no impact on another related protein, beta-secretase 2 (*BACE2*), also encoded on HSA21 but not previously associated with FMRP (Figure 4F). These data support the regulation of DS-implicated genes by FMRP.

FMRP upregulation is sufficient to reverse over 40% of the global transcriptional perturbations in hPSC models of DS

To identify additional gene and pathway perturbations in DS that could be modulated by FMRP upregulation using an unbiased approach, we next assessed the impact of FMRP CRISPRa induction on the global transcriptional landscape. Here, we analyzed the same isogenic cell lines and time-points used for candidate protein-level analyses in Figure 4, using four replicates per condition (Figures 5 and S3; Table S5). As expected, *FMR1* transcript levels were significantly upregulated upon 48 and 120 h FMRP CRISPRa induction and returned to baseline in the post-treatment condition (Figure S3). Looping back to targets that showed significant protein changes upon FMRP CRISPRa we noted that *DYRK1A* transcript levels were transiently increased at the 120 h time point (Figure S3), opposite the protein-level changes (Figure 4D), which could point to a compensatory increase in transcript abundance upon protein downregulation (Liu et al., 2018). *APP* transcript levels were transiently decreased by 48 h FMRP CRISPRa induction followed by a gradual recovery (Figure S3), roughly paralleling the observed protein-level changes (Figure 4E). We identified a total of 3,450 significant DEGs in the DS-CRISPRa (untreated) condition compared with the isogenic euploid control (Figures 5A–5C and S3; Table S5). FMRP upregulation alone was sufficient to reverse the directionality of 21% of those DEGs at both the 48 h time point (Figures 5A and S3; Table S5; 723/3450 DEGs) and the 120 h time point (Figures 5B and S3; Table S5; 725/3450 DEGs). By the post-treatment condition, 43% of all DEGs were reversed (Figures 5C and S3; Table S5; 1479/3450 DEGs), consistent with FMRP upregulation leading to both significant and sustained impacts on the global DS transcriptional program. As an example, 521 genes that were significantly upregulated in DS compared with euploid control were significantly downregulated post-treatment ($p = 4.7 \times 10^{-144}$), and 958 genes that were significantly downregulated in DS compared with euploid control were significantly upregulated post-treatment ($p = 7.7 \times 10^{-141}$; Figure 5C). Looping back to the DEGs shared between FXS and DS (Figure 3), we noted that *CHCHD2*, which was the most significant DEG in both the DS and FXS hPSC RNA-seq datasets, went from significantly downregulated in the untreated condition to significantly upregulated in the 120 h and post-treatment conditions (Table S5).

Focusing on all DEGs that reversed directionality in the post-treatment condition, the top 5 most significant canonical pathways included “transcriptional regulatory network in ESCs” and “DNA methylation and transcriptional repression signaling,” in addition to “wound healing signaling pathway,” indicating FMRP may be mediating changes in

DS through modulation of transcriptional networks in addition to other pathways (Figure 5D). Here, we noted examples of multiple collagen genes, including *collagen type VI alpha 3 chain (COL6A3)* relevant to the wound healing signaling pathway, which were downregulated in DS compared with euploid controls, and then upregulated by FMRP induction (Figure 5E; Table S5). We also identified multiple developmental transcription factors and epigenetic regulators, such as *HESX homeobox 1 (HESX1)*, *PR/SET domain 14 (PRDM14)*, and *nuclear receptor subfamily 5 group A member 2 (NR5A2)* relevant to the transcriptional regulatory network in ESCs and DNA methylation and transcriptional repression signaling pathways, which were upregulated in DS compared with euploid controls, and downregulated by FMRP induction (Figure 5E; Table S5). Additional examples of individual genes modulated in DS and reversed by FMRP induction are also shown across the full-time course in Figure S3. Note that for some DEGs that reversed directionality upon FMRP induction, the effects persisted post-treatment (Figure 5E) while others reverted to DS expression levels post-treatment (Figure S3).

Collectively, these analyses indicate that FMRP is capable of either directly or indirectly modulating a significant fraction of DS-implicated genes in *trans*.

DISCUSSION

These results provide evidence for the functional relevance of previous associations between FMRP targets and disease-implicated genes. They also underscore the need to probe the precise areas where gene set overlap may translate into convergent molecular mechanisms, given the diverse functions of FMRP in RNA processing, which may be at the level of protein abundance, transcript abundance, or additional mechanisms of transcript regulation, such as editing, splicing, or trafficking (Alpatov et al., 2014; Chakraborty et al., 2020; Chen et al., 2014; D'Souza et al., 2018; Darnell et al., 2011; Dichtenberg et al., 2008; Didiot et al., 2008; Edens et al., 2019; Kim et al., 2009; Kim et al., 2019; Tran et al., 2019; Tsang et al., 2019; Zhou et al., 2017). Indeed, the modest global transcriptional changes observed in FXS compared with DS may reflect the multiple layers of gene regulation perturbed by constitutive FMRP loss in addition to transcript abundance. In future studies, it will be critical to probe how gene set overlap between FXS and autism, schizophrenia, or bipolar disorder translates into potential molecular convergence.

Importantly, molecular overlap between disorders is one promising strategy to triangulate on impactful targets, which remains an enormous challenge. We hypothesize that genes with evidence for coordinate dysregulation in two or more disorders are more likely to play contributing roles to the disease biology. In the case of FXS, leveraging insights from other disorders with FMRP target overlap, such as DS, schizophrenia, or autism, may be a particularly useful strategy for target prioritization. For example, CBS upregulation in DS has established roles in mitochondrial dysfunction and cognitive deficits (Marechal et al., 2019; Panagaki et al., 2019; Szabo, 2020), and NCAM2 upregulation in DS has been shown to play a role in synaptic dysfunction (Sheng et al., 2018); given the relevance of these phenotypes in FXS, our data showing upregulated CBS and NCAM2 in FXS suggest that these genes are priority targets for additional investigation. While many gene targets and patient phenotypes do not overlap between DS and FXS, genes disrupted in

both diseases may be more likely to underlie the shared phenotypes, including cognitive dysfunction, deficits in expressive communication, or increased rates of autism, seizure disorders, and mental health disorders (Capone et al., 2006; Finestack et al., 2009; Jensen and Bulova, 2014; Martin et al., 2009; Tranfaglia, 2012). The consistent upregulation of some proteins like CBS across genetic backgrounds may indicate their involvement in more penetrant phenotypes, compared with NCAM2, whose expression levels varied with genetic background and may therefore contribute to more variable traits (Deutsch et al., 2005). Some of the gene perturbations we identified as shared between DS and FXS are also known to drive other neurodevelopmental disorders or phenotypes, which will be critical to probe in future studies.

Our data also support a causal relationship between FMRP and regulation of DS-implicated transcript targets reportedly bound by FMRP. At the candidate level, we observed downregulation of APP and DYRK1A upon FMRP induction. Using an unbiased approach, we found that FMRP induction was sufficient to either directly or indirectly modulate a significant fraction of DS gene perturbations in *trans*. Interestingly, many of the transcriptional changes in DS that were reversed by FMRP induction persisted after FMRP levels had returned to baseline, raising the possibility that FMRP mediates more stable epigenetic changes. Consistent with this notion, we identified terms related to transcriptional and methylation signaling using unbiased pathway analyses, and examples of individual transcriptional and epigenetic modifiers that were altered in response to FMRP induction. These data are consistent with previous studies of FXS that identify epigenetic modifiers as key downstream targets of FMRP (Shah et al., 2020). Our data showing that some transcripts in DS were upregulated following FMRP induction while others were downregulated is again consistent with diverse mechanisms of gene regulation. We speculate that a majority of the observed transcriptional effects of FMRP induction in DS were indirect (i.e., FMRP regulation of a transcription factor, which then impacts downstream gene expression as opposed to FMRP directly binding all differentially regulated transcripts). It is important to note that FMRP has many diverse transcript targets, and we would thus expect transcript and protein-level changes upon FMRP induction that are both related to, and unrelated to, DS or other neurodevelopmental disorders. We also note that acute upregulation of FMRP in the context of DS led to more transcriptional changes compared with constitutive loss of FMRP in euploid cells. Here, we speculate that acute modulation of FMRP may lead to more dramatic changes in gene regulation compared with constitutive modulation.

Taken together, our results identify specific areas of molecular convergence between DS and FXS using physiologically relevant human cellular models and provide evidence for the functional relevance of previous associations between FMRP targets and other disease-implicated genes. Broadly speaking, these findings support the hypothesis that neurodevelopmental disorders driven by distinct genetic alterations can converge on common molecular perturbations.

Limitations of the study

Our analyses are most relevant for early human development using *in vitro* systems but do not capture connections between DS and FXS in the more complex *in vivo* environment

or advanced developmental stages. Deficits due to loss of FMRP have been identified early in development, including in germ cells and embryos (Alpatov et al., 2014; Greenblatt and Spradling, 2018), as well as at later developmental stages, with longitudinal neuroimaging studies of patients with FXS pointing to abnormalities that implicate both pre- and postnatal processes (Hoeft et al., 2010). Studies of DS similarly implicate both pre- and postnatal deficits in the central nervous system (Haydar and Reeves, 2012). While early developmental stages are well suited to investigation using hPSC models, future studies will be required to fully elucidate connections between DS and FXS in later development and aging. Moreover, we focus on two specific cell types: hPSCs and glutamatergic neurons. Our analyses do not address other brain cell types, such as glia or interneurons, which may be highly relevant to disease pathology. Finally, we focus on the impacts of FMRP induction through CRISPRa specifically in the context of DS. Given the diverse functions of FMRP, it is almost certain that FMRP induction also impacts diverse pathways and phenotypes unrelated to DS.

STAR★METHODS

RESOURCE AVAILABILITY

Lead contact—Further information and requests for resources and reagents should be directed to and will be fulfilled by the lead contact, Lindy E. Barrett (lbarrett@broadinstitute.org).

Materials availability—Plasmids will be deposited in [Addgene.org](https://www.addgene.org) and generated cell lines will be made available upon request to the Lead Contact, following appropriate institutional approvals as well as regulations for cell line use and distribution.

Data and code availability

- RNA-seq datasets generated in this study have been deposited into NCBI GEO and are publicly available as of the date of publication. Accession numbers are listed in the key resources table.
- RNA-seq analysis codes utilized in this study have been deposited in Github and are publicly available as of the date of publication. A link is provided in the key resources table.
- Any additional information required to reanalyze data reported in this paper is available from the lead contact upon request.

EXPERIMENTAL MODEL AND SUBJECT DETAILS

Human pluripotent stem cell resources—All studies using hPSCs followed institutional IRB and ESCRO guidelines approved by Harvard University. The XY human embryonic stem cell line H1 was commercially obtained from WiCell Research Institute (Thomson et al., 1998) and used to generate isogenic *FMR1*^{+/+} and *FMR1*^{-/-} cell lines previously described (Susco et al., 2020). The XY human DS patient iPSC lines UWWC1-DS1, UWWC1-2DS3 and the euploid control UWWC1-DS2U (isogenic with UWWC1-DS1) were commercially obtained from WiCell Research Institute (Weick et al., 2013).

The control iPSC line CW60278 was obtained from the CIRM hPSC Repository funded by the California Institute of Regenerative Medicine (CIRM), at FujiFilm CDI. Three FXS patient iPSCs were reprogrammed at the Harvard Stem Cell Institute Core (Cambridge MA) with Sendai virus using XY patient fibroblasts. The following fibroblast cell lines were obtained from the NIGMS Human Genetic Cell Repository at the Coriell Institute for Medical Research: GM05131, GM04026 and GM09497, referred to as FXS iPSC A, FXS iPSC B and FXS iPSC C in this study, respectively, after reprogramming. XY cell lines were selected based on clinical data indicating that males are typically more severely affected by FXS than females and to avoid heterogeneity with respect to X chromosome inactivation in edited clones. Cell culture was carried out as previously described (Bara et al., 2016; Hazelbaker et al., 2017, 2020). In brief, stem cells were grown and maintained in mTeSR medium (Stem Cell Technologies) on geltrex-coated (Life Technologies) plates at 37° C. Cell lines underwent QC testing to confirm expected karyotypes and genotypes, absence of mycoplasma, expression of pluripotency markers and tri-lineage potential. G-band karyotyping analysis was performed by Cell Line Genetics.

METHOD DETAILS

CRISPR-Cas9 based genome engineering—To generate CRISPRa cell lines, TRE-dCas9-VPR-eGFP was inserted into the AAVS1 locus of the DS patient iPSC A (UWWC1-DS1) using TALENs, as previously described (Hazelbaker et al., 2020). Three gRNAs targeting *FMR1* for CRISPRa (g1: GCGCTGCTG GGAACCGGCCG, g2: CAGGTCGCACTGCCTCGCGA, g3: AGACCAGACACCCCTCCCG) were designed with the CRISPR-ERA tool (Liu et al., 2015), cloned into a multiplexed *piggyBac* vector and co-transfected in the presence of a *piggyBac* transposase, as previously described (Hazelbaker et al., 2020). Following selection with G418 and blasticidin, cells were assessed for EGFP+/mRFP + fluorescence and FMRP expression following doxycycline induction.

Generation of human glutamatergic neurons—Human neurons were generated as previously described (Nehme et al., 2018; Zhang et al., 2013). In brief, hPSCs were transduced with TetO-Ngn2-T2A-Puro and Ubiquitin-rtTA lentivirus or TetO-Ngn2-P2A-Zeo and CAG-rtTA were integrated into the AAVS1 safe-harbor locus using TALENs. Cells were then treated with doxycycline to induce ectopic Ngn2 expression combined with the extrinsic addition of SMAD inhibitors (SB431542, 1614, Tocris, and LDN-193189, 04-0074, Stemgent), Wnt inhibitors (XAV939, 04-0046, Stemgent) and neurotrophins (BDNF, GDNF, CNTF) followed by puromycin treatment to eliminate uninfected stem cells and maintenance in Neurobasal medium. Neurons were analyzed at day 14 of *in vitro* differentiation, a time point at which previous studies support connectivity and prenatal neuronal gene expression programs (Nehme et al., 2018; Susco et al., 2020). Ultra-high lentiviral titer was generated by Alstem, LLC.

RNA-seq of DS and FXS cell lines—RNA was extracted from hPSCs and neurons using the AllPrep DNA/RNA/miRNA Universal Kit (Qiagen) using five replicates per genotype and cell type. Sequencing libraries were prepared using the Illumina TruSeq HS Stranded Total RNA kit with Ribo-Zero Gold for rRNA depletion and quantified using the Agilent Bioanalyzer RNA Pico kit. Libraries were sequenced on a HiSeq

2500 at the Broad Institute Genomics Platform to generate 100bp paired end reads. RNA-seq QC and analysis was performed by the Harvard Chan Bioinformatics Core, Harvard T.H. Chan School of Public Health, Boston, MA. Reads were processed to counts through the bcbio RNA-seq pipeline implemented in the bcbio-nextgen project (<https://bcbio-nextgen.readthedocs.org/en/latest/>). Raw reads were examined for quality issues using FastQC (<http://www.bioinformatics.babraham.ac.uk/projects/fastqc/>) to ensure library generation and sequencing were suitable for further analysis. As necessary, adapter sequences, other contaminant sequences such as polyA tails and low quality sequences with PHRED quality scores less than five were trimmed from reads using cutadapt (Martin, 2011). Trimmed reads were aligned to Ensembl build GRCh38_90 of the Homo sapiens genome (human), using STAR (Dobin et al., 2013). Alignments were checked for evenness of coverage, rRNA content, genomic context of alignments (for example, alignments in known transcripts and introns), complexity and other quality checks using a combination of FastQC, Qualimap (Garcia-Alcalde et al., 2012), MultiQC (<https://github.com/ewels/MultiQC>) and custom tools. Counts of reads aligning to known genes were generated by featureCounts (Liao et al., 2014). In parallel, TPM measurements per isoform were generated by quasialignment using Salmon (Patro et al., 2015). Differential expression at the gene level was called with DESeq2 (Love et al., 2014), preferring to use counts per gene estimated from the Salmon quasialignments by tximport (Soneson et al., 2015). Quantitating at the isoform level has been shown to produce more accurate results at the gene level.

mRNA-seq of CRISPRa cell lines—RNA was extracted from hPSCs using the AllPrep DNA/RNA/miRNA Universal Kit (Qiagen) using four replicates per condition: DS2U Euploid Control, DS CRISPRa (untreated), DS 48hr FMRP CRISPRa, DS 120hr FMRP CRISPRa and DS 120hr on/120hr off FMRP CRISPRa. Libraries were prepared using Roche Kapa mRNA HyperPrep strand specific sample preparation kits from 200ng of purified total RNA according to the manufacturer's protocol on a Beckman Coulter Biomek i7. The finished dsDNA libraries were quantified by Qubit fluorometer and Agilent TapeStation 4200. Uniquely dual indexed libraries were pooled in equimolar ratio and shallowly sequenced on an Illumina MiSeq to further evaluate library quality and pooling balance. The final pool was sequenced on an Illumina NovaSeq 6000 targeting 30 million 100bp read pairs per library. Sequenced reads were aligned to the UCSC hg19 reference genome assembly and gene counts were quantified using STAR (v2.7.3a) (Dobin et al., 2013). Differential gene expression testing was performed by DESeq2 (v1.22.1) (Love et al., 2014). RNAseq analysis was performed using the VIPER snakemake pipeline (Cornwell et al., 2018). Library preparation, Illumina sequencing and VIPER workflow were performed by the Dana-Farber Cancer Institute Molecular Biology Core Facilities.

Western Blot analyses—Cells were lysed using RIPA lysis buffer (Life Technologies) with protease inhibitors (cOmplete, Mini, EDTA-free Protease Inhibitor Cocktail, Roche). 20ug of protein as determined by Peirce BCA Protein Assay kit (Thermo Scientific) was loaded onto Bolt 4–12% Bis-Tris Plus gels (Invitrogen), transferred using the iBlot2 system (Thermo Scientific), blocked in 5% milk in TBST, and then incubated with primary antibodies in 1% milk in TBST overnight at 4°C. Membranes were rinsed in TBST, incubated with secondary antibodies for 1 h at room temperature, rinsed in TBST, and

then developed using SuperSignal West Femto Maximum Sensitivity Substrate (Thermo Scientific). The following primary antibodies were used: anti-FMRP (Abcam ab17722), anti-GAPDH (EMD MAB374), anti-NCAM2 (Abcam ab173297), anti-DYRK1A (Bethyl A303–802A), anti-FXR1P (ML13 courtesy E. Khandjian), anti-CBS (Proteintech 14787–1-AP), anti-APP (Abcam ab32136) and anti-BACE2 (Abcam ab270458). For quantification, bands were analyzed in FIJI, normalized to GAPDH, averaged, and plotted with SEM for error bars. All Western blots were performed on triplicate samples and significance was calculated by unpaired two-tailed t test for comparisons between two groups. Prism (GraphPad Software) was used for statistical analyses.

QUANTIFICATION AND STATISTICAL ANALYSIS

Replicates for experiments using hPSCs refer to separate wells or plates and replicates for experiments using neurons refer to independent neuronal differentiations. For RNA-seq analyses of DS and FXS cell lines, we used an adjusted p value cutoff of 0.05. For mRNA-seq of CRISPRa lines, a \log_2 foldchange cutoff of over 1 or under -1 was also applied. For Western blot analyses, experiments were performed on triplicate samples and significance was calculated by unpaired two-tailed t test for comparisons between two groups; Prism (GraphPad Software) was used for statistical analyses. For statistical tests of enrichment and overlap, we used the hypergeometric test for over- or under-enrichment. To determine the size of the RNA universe in both hPSCs and neurons, we looked at the TPM counts from the RNA-seq data and counted a gene as expressed if it had an average TPM ≥ 1 across five replicates in each control cell type. This generated 15,316 RNAs expressed in neurons, and 14,233 RNAs expressed in hPSCs. p values (or adjusted p values, where applicable) < 0.05 were considered statistically significant.

Supplementary Material

Refer to Web version on PubMed Central for supplementary material.

ACKNOWLEDGMENTS

We thank members of the Barrett lab for insightful discussions and critical reading of the manuscript. We also thank Ajamete Kaykas and Katie Worringer for the Ngn2 *AAVS1* targeting construct. We thank Edouard Khandjian for the ML13 anti-FXR1P antibody. We appreciate the analytical support from Zach Herbert at the Dana-Farber Cancer Institute Molecular Biology Core Facilities. iPSC reprogramming was performed at the Harvard Stem Cell Institute iPSC core facility (Cambridge, MA). This work was supported by NIH grants R21MH109761 and R01HD101534 to L.E.B. as well as support from the Stanley Center for Psychiatric Research. Work done by V.B. at the Harvard Chan Bioinformatics Core was partially supported by Harvard Catalyst, the Harvard Clinical and Translational Science Center (National Center for Advancing Translational Sciences, National Institutes of Health Award UL1TR002541), and financial contributions from Harvard University and its affiliated academic healthcare centers; the content is solely the responsibility of the authors and does not necessarily represent the official views of Harvard Catalyst, Harvard University and its affiliated academic healthcare centers, or the National Institutes of Health.

REFERENCES

Alpatov R, Lesch BJ, Nakamoto-Kinoshita M, Blanco A, Chen S, Stützer A, Armache KJ, Simon MD, Xu C, Ali M, et al. (2014). A chromatin-dependent role of the fragile X mental retardation protein FMRP in the DNA damage response. *Cell* 157, 869–881. 10.1016/j.cell.2014.03.040. [PubMed: 24813610]

- Bagni C, Tassone F, Neri G, and Hagerman R (2012). Fragile X syndrome: causes, diagnosis, mechanisms, and therapeutics. *J. Clin. Invest* 122, 4314–4322. 10.1172/JCI63141. [PubMed: 23202739]
- Bara AM, Messana A, Herring A, Hazelbaker DZ, Eggan K, and Barrett LE (2016). Generation of a TLE3 heterozygous knockout human embryonic stem cell line using CRISPR-Cas9. *Stem Cell Res.* 17, 441–443. 10.1016/j.scr.2016.09.008. [PubMed: 27879221]
- Capone G, Goyal P, Ares W, and Lannigan E (2006). Neurobehavioral disorders in children, adolescents, and young adults with Down syndrome. *Am. J. Med. Genet. C Semin. Med. Genet* 142C, 158–172. 10.1002/ajmg.c.30097. [PubMed: 16838318]
- Chakraborty A, Jenjaroenpun P, Li J, El Hilali S, McCulley A, Haarer B, Hoffman EA, Belak A, Thorland A, Hehny H, et al. (2020). Replication stress induces global chromosome breakage in the fragile X genome. *Cell Rep.* 32, 108179. 10.1016/j.celrep.2020.108179.
- Chanda S, Ang CE, Lee QY, Ghebrial M, Haag D, Shibuya Y, Wernig M, and Südhof TC (2019). Direct reprogramming of human neurons identifies MARCKSL1 as a pathogenic mediator of valproic acid-induced teratogenicity. *Cell Stem Cell* 25, 103–119.e6. 10.1016/j.stem.2019.04.021. [PubMed: 31155484]
- Chen E, Sharma MR, Shi X, Agrawal RK, and Joseph S (2014). Fragile X mental retardation protein regulates translation by binding directly to the ribosome. *Mol. Cell* 54, 407–417. 10.1016/j.molcel.2014.03.023. [PubMed: 24746697]
- Clifton NE, Rees E, Holmans PA, Pardiñas AF, Harwood JC, Di Florio A, Kirov G, Walters JTR, O'Donovan MC, Owen MJ, et al. (2020). Genetic association of FMRP targets with psychiatric disorders. *Mol. Psychiatr* 26, 2977–2990. 10.1038/s41380-020-00912-2.
- Cornwell M, Vangala M, Taing L, Herbert Z, Köster J, Li B, Sun H, Li T, Zhang J, Qiu X, et al. (2018). VIPER: visualization Pipeline for RNA-seq, a Snakemake workflow for efficient and complete RNA-seq analysis. *BMC Bio-inf.* 19, 135. 10.1186/s12859-018-2139-9.
- Courcet JB, Faivre L, Malzac P, Masurel-Paulet A, Lopez E, Callier P, Lambert L, Lemesle M, Thevenon J, Gigot N, et al. (2012). The DYRK1A gene is a cause of syndromic intellectual disability with severe microcephaly and epilepsy. *J. Med. Genet* 49, 731–736. 10.1136/jmedgenet-2012-101251. [PubMed: 23099646]
- D'Antoni S, de Bari L, Valenti D, Borro M, Bonaccorso CM, Simmaco M, Vacca RA, and Catania MV (2020). Aberrant mitochondrial bioenergetics in the cerebral cortex of the Fmr1 knockout mouse model of fragile X syndrome. *Biol. Chem* 401, 497–503. 10.1515/hsz-2019-0221. [PubMed: 31702995]
- D'Souza MN, Gowda NKC, Tiwari V, Babu RO, Anand P, Dastidar SG, Singh R, James OG, Selvaraj B, Pal R, et al. (2018). FMRP interacts with C/D box snoRNA in the nucleus and regulates ribosomal RNA methylation. *iScience* 9, 399–411. 10.1016/j.isci.2018.11.007. [PubMed: 30469012]
- Darnell JC, Van Driesche SJ, Zhang C, Hung KYS, Mele A, Fraser CE, Stone EF, Chen C, Fak JJ, Chi SW, et al. (2011). FMRP stalls ribosomal translocation on mRNAs linked to synaptic function and autism. *Cell* 146, 247–261. 10.1016/j.cell.2011.06.013. [PubMed: 21784246]
- Davis JK, and Broadie K (2017). Multifarious functions of the fragile X mental retardation protein. *Trends Genet.* 33, 703–714. 10.1016/j.tig.2017.07.008. [PubMed: 28826631]
- de la Torre R, de Sola S, Hernandez G, Farré M, Pujol J, Rodriguez J, Espadaler JM, Langohr K, Cuenca-Royo A, Principe A, et al. (2016). Safety and efficacy of cognitive training plus epigallocatechin-3-gallate in young adults with Down's syndrome (TESDAD): a double-blind, randomised, placebo-controlled, phase 2 trial. *Lancet Neurol.* 15, 801–810. 10.1016/S1474-4422(16)30034-5. [PubMed: 27302362]
- De Toma I, Manubens-Gil L, Ossowski S, and Dierssen M (2016). Where environment meets cognition: a focus on two developmental intellectual disability disorders. *Neural Plast.* 2016, 4235898. 10.1155/2016/4235898.
- Deciphering Developmental Disorders Study (2017). Prevalence and architecture of de novo mutations in developmental disorders. *Nature* 542, 433–438. 10.1038/nature21062. [PubMed: 28135719]
- Del Hoyo Soriano L, Thurman AJ, Harvey D, Kover ST, and Abbeduto L (2020). Expressive language development in adolescents with Down syndrome and fragile X syndrome: change over time

and the role of family-related factors. *J. Neurodev. Disord* 12, 18. 10.1186/s11689-020-09320-7. [PubMed: 32593286]

- Deutsch S, Lyle R, Dermitzakis ET, Attar H, Subrahmanyam L, Gehrig C, Parand L, Gagnebin M, Rougemont J, Jongeneel CV, and Antonarakis SE (2005). Gene expression variation and expression quantitative trait mapping of human chromosome 21 genes. *Hum. Mol. Genet* 14, 3741–3749. 10.1093/hmg/ddi404. [PubMed: 16251198]
- Dicthenberg JB, Swanger SA, Antar LN, Singer RH, and Bassell GJ (2008). A direct role for FMRP in activity-dependent dendritic mRNA transport links filopodial-spine morphogenesis to fragile X syndrome. *Dev. Cell* 14, 926–939. 10.1016/j.devcel.2008.04.003. [PubMed: 18539120]
- Didiot MC, Tian Z, Schaeffer C, Subramanian M, Mandel JL, and Moine H (2008). The G-quartet containing FMRP binding site in FMR1 mRNA is a potent exonic splicing enhancer. *Nucleic Acids Res.* 36, 4902–4912. 10.1093/nar/gkn472. [PubMed: 18653529]
- Dobin A, Davis CA, Schlesinger F, Drenkow J, Zaleski C, Jha S, Batut P, Chaisson M, and Gingeras TR (2013). STAR: ultrafast universal RNA-seq aligner. *Bioinformatics* 29, 15–21. 10.1093/bioinformatics/bts635. [PubMed: 23104886]
- Doran E, Keator D, Head E, Phelan MJ, Kim R, Totoiu M, Barrio JR, Small GW, Potkin SG, and Lott IT (2017). Down syndrome, partial trisomy 21, and absence of alzheimer’s disease: the role of APP. *J. Alzheimers Dis* 56, 459–470. 10.3233/JAD-160836. [PubMed: 27983553]
- Duchon A, and Hérault Y (2016). DYRK1A, a dosage-sensitive gene involved in neurodevelopmental disorders, is a target for drug development in Down syndrome. *Front. Behav. Neurosci* 10, 104. 10.3389/fnbeh.2016.00104. [PubMed: 27375444]
- Edens BM, Vissers C, Su J, Arumugam S, Xu Z, Shi H, Miller N, Rojas Ringeling F, Ming GL, He C, et al. (2019). FMRP modulates neural differentiation through m(6)a-dependent mRNA nuclear export. *Cell Rep.* 28, 845–854.e5. 10.1016/j.celrep.2019.06.072. [PubMed: 31340148]
- Faundez V, De Toma I, Bardoni B, Bartesaghi R, Nizetic D, de la Torre R, Cohen Kadosh R, Hérault Y, Dierssen M, and Potier MC; Down Syndrome and Other Genetic Developmental Disorders ECNP Network (2018). Translating molecular advances in Down syndrome and Fragile X syndrome into therapies. *Eur. Neuropsychopharmacol* 28, 675–690. 10.1016/j.euroneuro.2018.03.006. [PubMed: 29887288]
- Finestack LH, Richmond EK, and Abbeduto L (2009). Language development in individuals with fragile X syndrome. *Top. Lang. Disord* 29, 133–148. [PubMed: 20396595]
- García-Alcalde F, Okonechnikov K, Carbonell J, Cruz LM, Götz S, Tarazona S, Dopazo J, Meyer TF, and Conesa A (2012). Qualimap: evaluating next-generation sequencing alignment data. *Bioinformatics* 28, 2678–2679. 10.1093/bioinformatics/bts503. [PubMed: 22914218]
- Garshasbi M, Hadavi V, Habibi H, Kahrizi K, Kariminejad R, Behjati F, Tzschach A, Najmabadi H, Ropers HH, and Kuss AW (2008). A defect in the TUSC3 gene is associated with autosomal recessive mental retardation. *Am. J. Hum. Genet* 82, 1158–1164. 10.1016/j.ajhg.2008.03.018. [PubMed: 18452889]
- Germain PL, and Testa G (2017). Taming human genetic variability: transcriptomic meta-analysis guides the experimental design and interpretation of iPSC-based disease modeling. *Stem Cell Rep.* 8, 1784–1796. 10.1016/j.stemcr.2017.05.012.
- Greenblatt EJ, and Spradling AC (2018). Fragile X mental retardation 1 gene enhances the translation of large autism-related proteins. *Science* 361, 709–712. 10.1126/science.aas9963. [PubMed: 30115809]
- Haas MA, Bell D, Slender A, Lana-Elola E, Watson-Scales S, Fisher EMC, Tybulewicz VLJ, and Guillemot F (2013). Alterations to dendritic spine morphology, but not dendrite patterning, of cortical projection neurons in Tc1 and Ts1Rhr mouse models of Down syndrome. *PLoS One* 8, e78561. 10.1371/journal.pone.0078561.
- Han MR, Schellenberg GD, and Wang LS; Alzheimer’s Disease Neuroimaging Initiative (2010). Genome-wide association reveals genetic effects on human Abeta42 and tau protein levels in cerebrospinal fluids: a case control study. *BMC Neurol.* 10, 90. 10.1186/1471-2377-10-90. [PubMed: 20932310]
- Haydar TF, and Reeves RH (2012). Trisomy 21 and early brain development. *Trends Neurosci.* 35, 81–91. 10.1016/j.tins.2011.11.001. [PubMed: 22169531]

- Hazelbaker DZ, Beccard A, Angelini G, Mazzucato P, Messana A, Lam D, Eggen K, and Barrett LE (2020). A multiplexed gRNA piggyBac transposon system facilitates efficient induction of CRISPRi and CRISPRa in human pluripotent stem cells. *Sci. Rep* 10, 635. 10.1038/s41598-020-57500-1. [PubMed: 31959800]
- Hazelbaker DZ, Beccard A, Bara AM, Dabkowski N, Messana A, Mazzucato P, Lam D, Manning D, Eggen K, and Barrett LE (2017). A scaled framework for CRISPR editing of human pluripotent stem cells to study psychiatric disease. *Stem Cell Rep.* 9, 1315–1327. 10.1016/j.stemcr.2017.09.006.
- Hibaoui Y, Grad I, Letourneau A, Sailani MR, Dahoun S, Santoni FA, Gimelli S, Guipponi M, Pelte MF, Béna F, et al. (2014). Modelling and rescuing neurodevelopmental defect of Down syndrome using induced pluripotent stem cells from monozygotic twins discordant for trisomy 21. *EMBO Mol. Med* 6, 259–277. 10.1002/emmm.201302848. [PubMed: 24375627]
- Hoeffler CA, Sanchez E, Hagerman RJ, Mu Y, Nguyen DV, Wong H, Whelan AM, Zukin RS, Klann E, and Tassone F (2012). Altered mTOR signaling and enhanced CYFIP2 expression levels in subjects with fragile X syndrome. *Gene Brain Behav.* 11, 332–341. 10.1111/j.1601-183X.2012.00768.x.
- Hoelt F, Carter JC, Lightbody AA, Cody Hazlett H, Piven J, and Reiss AL (2010). Region-specific alterations in brain development in one- to three-year-old boys with fragile X syndrome. *Proc. Natl. Acad. Sci. USA* 107, 9335–9339. 10.1073/pnas.1002762107. [PubMed: 20439717]
- Hoffman GE, Schrode N, Flaherty E, and Brennand KJ (2019). New considerations for hiPSC-based models of neuropsychiatric disorders. *Mol. Psychiatr* 24, 49–66. 10.1038/s41380-018-0029-1.
- Iossifov I, O’Roak BJ, Sanders SJ, Ronemus M, Krumm N, Levy D, Stessman HA, Witherspoon KT, Vives L, Patterson KE, et al. (2014). The contribution of de novo coding mutations to autism spectrum disorder. *Nature* 515, 216–221. 10.1038/nature13908. [PubMed: 25363768]
- Jacquemont S, Pacini L, Jønch AE, Cencelli G, Rozenberg I, He Y, D’Andrea L, Pedini G, Eldeeb M, Willemsen R, et al. (2018). Protein synthesis levels are increased in a subset of individuals with fragile X syndrome. *Hum. Mol. Genet* 27, 3825. 10.1093/hmg/ddy291. [PubMed: 30107584]
- Jensen KM, and Bulova PD (2014). Managing the care of adults with Down’s syndrome. *BMJ* 349, g5596. 10.1136/bmj.g5596. [PubMed: 25269800]
- Joseph RM (2014). Neuronatin gene: imprinted and misfolded: studies in Lafora disease, diabetes and cancer may implicate NNAT-aggregates as a common downstream participant in neuronal loss. *Genomics* 103, 183–188. 10.1016/j.ygeno.2013.12.001. [PubMed: 24345642]
- Kang Y, Zhou Y, Li Y, Han Y, Xu J, Niu W, Li Z, Liu S, Feng H, Huang W, et al. (2021). A human forebrain organoid model of fragile X syndrome exhibits altered neurogenesis and highlights new treatment strategies. *Nat. Neurosci* 24, 1377–1391. 10.1038/s41593-021-00913-6. [PubMed: 34413513]
- Kee TR, Espinoza Gonzalez P, Wehinger JL, Bukhari MZ, Ermekbaeva A, Sista A, Kotsiviras P, Liu T, Kang DE, and Woo JAA (2021). Mitochondrial CHCHD2: disease-associated mutations, physiological functions, and current animal models. *Front. Aging Neurosci* 13, 660843. 10.3389/fnagi.2021.660843.
- Khalfallah O, Jarjat M, Davidovic L, Nottet N, Cestèle S, Mantegazza M, and Bardoni B (2017). Depletion of the fragile X mental retardation protein in embryonic stem cells alters the kinetics of neurogenesis. *Stem Cell.* 35, 374–385. 10.1002/stem.2505.
- Kim M, Bellini M, and Ceman S (2009). Fragile X mental retardation protein FMRP binds mRNAs in the nucleus. *Mol. Cell Biol* 29, 214–228. 10.1128/MCB.01377-08. [PubMed: 18936162]
- Kim TH, Tsang B, Vernon RM, Sonenberg N, Kay LE, and Forman-Kay JD (2019). Phospho-dependent phase separation of FMRP and CAPRIN1 recapitulates regulation of translation and deadenylation. *Science* 365, 825–829. 10.1126/science.aax4240. [PubMed: 31439799]
- Kimura R, Kamino K, Yamamoto M, Nuripa A, Kida T, Kazui H, Hashimoto R, Tanaka T, Kudo T, Yamagata H, et al. (2007). The DYRK1A gene, encoded in chromosome 21 Down syndrome critical region, bridges between beta-amyloid production and tau phosphorylation in Alzheimer disease. *Hum. Mol. Genet* 16, 15–23. 10.1093/hmg/ddl437. [PubMed: 17135279]

- Leshchyns'ka I, Liew HT, Shepherd C, Halliday GM, Stevens CH, Ke YD, Ittner LM, and Sytnyk V (2015). Abeta-dependent reduction of NCAM2-mediated synaptic adhesion contributes to synapse loss in Alzheimer's disease. *Nat. Commun* 6, 8836. 10.1038/ncomms9836. [PubMed: 26611261]
- Liao Y, Smyth GK, and Shi W (2014). featureCounts: an efficient general purpose program for assigning sequence reads to genomic features. *Bioinformatics* 30, 923–930. 10.1093/bioinformatics/btt656. [PubMed: 24227677]
- Lin YT, Seo J, Gao F, Feldman HM, Wen HL, Penney J, Cam HP, Gjonjeska E, Raja WK, Cheng J, et al. (2018). APOE4 causes widespread molecular and cellular alterations associated with alzheimer's disease phenotypes in human iPSC-derived brain cell types. *Neuron* 98, 1141–1154.e7. 10.1016/j.neuron.2018.05.008. [PubMed: 29861287]
- Liu B, Li Y, Stackpole EE, Novak A, Gao Y, Zhao Y, Zhao X, and Richter JD (2018). Regulatory discrimination of mRNAs by FMRP controls mouse adult neural stem cell differentiation. *Proc. Natl. Acad. Sci. USA* 115, E11397–E11405. 10.1073/pnas.1809588115. [PubMed: 30373821]
- Liu H, Wei Z, Dominguez A, Li Y, Wang X, and Qi LS (2015). CRISPR-ERA: a comprehensive design tool for CRISPR-mediated gene editing, repression and activation. *Bioinformatics* 31, 3676–3678. 10.1093/bioinformatics/btv423. [PubMed: 26209430]
- Lockstone HE, Harris LW, Swatton JE, Wayland MT, Holland AJ, and Bahn S (2007). Gene expression profiling in the adult Down syndrome brain. *Genomics* 90, 647–660. 10.1016/j.ygeno.2007.08.005. [PubMed: 17950572]
- Love MI, Huber W, and Anders S (2014). Moderated estimation of fold change and dispersion for RNA-seq data with DESeq2. *Genome Biol.* 15, 550. 10.1186/s13059-014-0550-8. [PubMed: 25516281]
- Marechal D, Brault V, Leon A, Martin D, Lopes Pereira P, Loaec N, Birling MC, Friocourt G, Blondel M, and Herault Y (2019). Cbs overdosage is necessary and sufficient to induce cognitive phenotypes in mouse models of Down syndrome and interacts genetically with Dyrk1a. *Hum. Mol. Genet* 28, 1561–1577. 10.1093/hmg/ddy447. [PubMed: 30649339]
- Martin GE, Klusek J, Estigarribia B, and Roberts JE (2009). Language characteristics of individuals with Down syndrome. *Top. Lang. Disord* 29, 112–132. [PubMed: 20428477]
- Martin M (2011). Cutadapt Removes Adapter Sequences from High-Throughput Sequencing Reads. *EMBnet. journal* 17, 10–12. 10.14806/ej.17.1.200.
- Martínez-Cerdeño V (2017). Dendrite and spine modifications in autism and related neurodevelopmental disorders in patients and animal models. *Dev. Neurobiol* 77, 393–404. 10.1002/dneu.22417. [PubMed: 27390186]
- Mateos MK, Barbaric D, Byatt SA, Sutton R, and Marshall GM (2015). Down syndrome and leukemia: insights into leukemogenesis and translational targets. *Transl. Pediatr* 4, 76–92. 10.3978/j.issn.2224-4336.2015.03.03. [PubMed: 26835364]
- Mattioli F, Hayot G, Drouot N, Isidor B, Courraud J, Hinckelmann MV, Mau-Them FT, Sellier C, Goldman A, Telegrafi A, et al. (2020). De novo frameshift variants in the neuronal splicing factor NOVA2 result in a common C-terminal extension and cause a severe form of neurodevelopmental disorder. *Am. J. Hum. Genet* 106, 438–452. 10.1016/j.ajhg.2020.02.013. [PubMed: 32197073]
- Mouton-Liger F, Thomas S, Rattenbach R, Magnol L, Larigaldie V, Ledru A, Herault Y, Verney C, and Créau N (2011). PCP4 (PEP19) overexpression induces premature neuronal differentiation associated with Ca(2+)/calmodulin-dependent kinase II-delta activation in mouse models of Down syndrome. *J. Comp. Neurol* 519, 2779–2802. 10.1002/cne.22651. [PubMed: 21491429]
- Nehme R, Zuccaro E, Ghosh SD, Li C, Sherwood JL, Pietilainen O, Barrett LE, Limone F, Worringer KA, Kommineni S, et al. (2018). Combining NGN2 programming with developmental patterning generates human excitatory neurons with NMDAR-mediated synaptic transmission. *Cell Rep.* 23, 2509–2523. [PubMed: 29791859]
- O'Roak BJ, Vives L, Fu W, Egerton JD, Stanaway IB, Phelps IG, Carvill G, Kumar A, Lee C, Ankenman K, et al. (2012). Multiplex targeted sequencing identifies recurrently mutated genes in autism spectrum disorders. *Science* 338, 1619–1622. 10.1126/science.1227764. [PubMed: 23160955]
- Pak C, Danko T, Zhang Y, Aoto J, Anderson G, Maxeiner S, Yi F, Wernig M, and Südhof TC (2015). Human neuropsychiatric disease modeling using conditional deletion reveals synaptic

- transmission defects caused by heterozygous mutations in NRXN1. *Cell Stem Cell* 17, 316–328. 10.1016/j.stem.2015.07.017. [PubMed: 26279266]
- Panagaki T, Randi EB, Augsburger F, and Szabo C (2019). Overproduction of H2S, generated by CBS, inhibits mitochondrial Complex IV and suppresses oxidative phosphorylation in Down syndrome. *Proc. Natl. Acad. Sci. USA* 116, 18769–18771. 10.1073/pnas.1911895116. [PubMed: 31481613]
- Patro R, Duggal G, and Kingsford C (2015). Accurate, fast, and model-aware transcript expression quantification with salmon. Preprint at bioRxiv. 10.1101/021592.
- Petit F, Plessis G, Decamp M, Cuisset JM, Blyth M, Pendlebury M, and Andrieux J (2015). 21q21 deletion involving NCAM2: report of 3 cases with neurodevelopmental disorders. *Eur. J. Med. Genet* 58, 44–46. 10.1016/j.ejmg.2014.11.004. [PubMed: 25464110]
- Prandini P, Deutsch S, Lyle R, Gagnebin M, Delucinge Vivier C, Delorenzi M, Gehrig C, Descombes P, Sherman S, Dagna Bricarelli F, et al. (2007). Natural gene-expression variation in Down syndrome modulates the outcome of gene-dosage imbalance. *Am. J. Hum. Genet* 81, 252–263. 10.1086/519248. [PubMed: 17668376]
- Raj N, McEachin ZT, Harousseau W, Zhou Y, Zhang F, Merritt-Garza ME, Taliaferro JM, Kalinowska M, Marro SG, Hales CM, et al. (2021). Cell-type-specific profiling of human cellular models of fragile X syndrome reveal PI3K-dependent defects in translation and neurogenesis. *Cell Rep.* 35, 108991. 10.1016/j.celrep.2021.108991.
- Raveau M, Nakahari T, Asada S, Ishihara K, Amano K, Shimohata A, Sago H, and Yamakawa K (2017). Brain ventriculomegaly in Down syndrome mice is caused by Pcp4 dose-dependent cilia dysfunction. *Hum. Mol. Genet* 26, 923–931. 10.1093/hmg/ddx007. [PubMed: 28069794]
- Rouhani F, Kumasaka N, de Brito MC, Bradley A, Vallier L, and Gaffney D (2014). Genetic background drives transcriptional variation in human induced pluripotent stem cells. *PLoS Genet.* 10, e1004432. 10.1371/journal.pgen.1004432.
- Sanders SJ, He X, Willsey AJ, Ercan-Sencicek AG, Samocha KE, Cicek AE, Murtha MT, Bal VH, Bishop SL, Dong S, et al. (2015). Insights into autism spectrum disorder genomic architecture and biology from 71 risk loci. *Neuron* 87, 1215–1233. 10.1016/j.neuron.2015.09.016. [PubMed: 26402605]
- Satterstrom FK, Kosmicki JA, Wang J, Breen MS, De Rubeis S, An JY, Peng M, Collins R, Grove J, Klei L, et al. (2020). Large-scale exome sequencing study implicates both developmental and functional changes in the neurobiology of autism. *Cell* 180, 568–584.e23. 10.1016/j.cell.2019.12.036. [PubMed: 31981491]
- Schizophrenia Working Group of the Psychiatric Genomics Consortium (2014). Biological insights from 108 schizophrenia-associated genetic loci. *Nature* 511, 421–427. 10.1038/nature13595. [PubMed: 25056061]
- Shah S, Molinaro G, Liu B, Wang R, Huber KM, and Richter JD (2020). FMRP control of ribosome translocation promotes chromatin modifications and alternative splicing of neuronal genes linked to autism. *Cell Rep.* 30, 4459–4472.e6. 10.1016/j.celrep.2020.02.076. [PubMed: 32234480]
- Sheng L, Leshchyns'ka I, and Sytnyk V (2018). Neural cell adhesion molecule 2 (NCAM2)-Induced c-src-dependent propagation of submembrane Ca²⁺ spikes along dendrites inhibits synapse maturation. *Cerebr. Cortex* 29, 1439–1459. 10.1093/cercor/bhy041.
- Soneson C, Love MI, and Robinson MD (2015). Differential analyses for RNA-seq: transcript-level estimates improve gene-level inferences. *F1000Res.* 4, 1521. 10.12688/f1000research.7563.2. [PubMed: 26925227]
- Sun AX, Yuan Q, Fukuda M, Yu W, Yan H, Lim GGY, Nai MH, D'Agostino GA, Tran HD, Itahana Y, et al. (2019). Potassium channel dysfunction in human neuronal models of Angelman syndrome. *Science* 366, 1486–1492. 10.1126/science.aav5386. [PubMed: 31857479]
- Susco SG, Arias-García MA, López-Huerta VG, Beccard A, Bara AM, Moffitt J, Korn J, Fu Z, and Barrett LE (2020). FMR1 loss in a human stem cell model reveals early changes to intrinsic membrane excitability. *Dev. Biol* 468, 93–100. 10.1016/j.ydbio.2020.09.012. [PubMed: 32976839]
- Szabo C (2020). The re-emerging pathophysiological role of the cystathionine-beta-synthase - hydrogen sulfide system in Down syndrome. *FEBS J.* 287, 3150–3160. 10.1111/febs.15214. [PubMed: 31955501]

- Tew J, and Goate AM (2017). Genetics of beta-amyloid precursor protein in alzheimer's disease. *Cold Spring Harb. Perspect. Med* 7, a024539. 10.1101/cshperspect.a024539.
- Teller JK, Russo C, DeBusk LM, Angelini G, Zaccheo D, Dagna-Bricarelli F, Scartezzini P, Bertolini S, Mann DM, Tabaton M, and Gambetti P (1996). Presence of soluble amyloid beta-peptide precedes amyloid plaque formation in Down's syndrome. *Nat. Med* 2, 93–95. 10.1038/nm0196-93. [PubMed: 8564851]
- Thomson JA, Itskovitz-Eldor J, Shapiro SS, Waknitz MA, Swiergiel JJ, Marshall VS, and Jones JM (1998). Embryonic stem cell lines derived from human blastocysts. *Science* 282, 1145–1147. [PubMed: 9804556]
- Tran SS, Jun HI, Bahn JH, Azghadi A, Ramaswami G, Van Nostrand EL, Nguyen TB, Hsiao YHE, Lee C, Pratt GA, et al. (2019). Widespread RNA editing dysregulation in brains from autistic individuals. *Nat. Neurosci* 22, 25–36. 10.1038/s41593-018-0287-x. [PubMed: 30559470]
- Tranfaglia MR (2012). Fragile X syndrome: a psychiatric perspective. *Results Probl. Cell Differ* 54, 281–295. 10.1007/978-3-642-21649-7_16. [PubMed: 22009359]
- Tsang B, Arsenault J, Vernon RM, Lin H, Sonenberg N, Wang LY, Bah A, and Forman-Kay JD (2019). Phosphoregulated FMRP phase separation models activity-dependent translation through bidirectional control of mRNA granule formation. *Proc. Natl. Acad. Sci. USA* 116, 4218–4227. 10.1073/pnas.1814385116. [PubMed: 30765518]
- Tsurusaki Y, Koshimizu E, Ohashi H, Phadke S, Kou I, Shiina M, Suzuki T, Okamoto N, Imamura S, Yamashita M, et al. (2014). De novo SOX11 mutations cause Coffin-Siris syndrome. *Nat. Commun* 5, 4011. 10.1038/ncomms5011. [PubMed: 24886874]
- Utami KH, Yusof NABM, Kwa JE, Peteri UK, Castrén ML, and Pouladi MA (2020). Elevated de novo protein synthesis in FMRP-deficient human neurons and its correction by metformin treatment. *Mol. Autism* 11, 41. 10.1186/s13229-020-00350-5. [PubMed: 32460900]
- Weick JP, Held DL, Bonadurer GF 3rd, Doers ME, Liu Y, Maguire C, Clark A, Knackert JA, Molinarolo K, Musser M, et al. (2013). Deficits in human trisomy 21 iPSCs and neurons. *Proc. Natl. Acad. Sci. USA* 110, 9962–9967. 10.1073/pnas.1216575110. [PubMed: 23716668]
- Weisz ED, Towheed A, Monyak RE, Toth MS, Wallace DC, and Jongens TA (2018). Loss of Drosophila FMRP leads to alterations in energy metabolism and mitochondrial function. *Hum. Mol. Genet* 27, 95–106. 10.1093/hmg/ddx387. [PubMed: 29106525]
- Westmark CJ, Chuang SC, Hays SA, Filon MJ, Ray BC, Westmark PR, Gibson JR, Huber KM, and Wong RKS (2016). APP causes hyper-excitability in fragile X mice. *Front. Mol. Neurosci* 9, 147. 10.3389/fnmol.2016.00147. [PubMed: 28018172]
- Westmark CJ, Westmark PR, O'Riordan KJ, Ray BC, Hervey CM, Salamat MS, Abozeid SH, Stein KM, Stodola LA, Tranfaglia M, et al. (2011). Reversal of fragile X phenotypes by manipulation of AbetaPP/Abeta levels in Fmr1KO mice. *PLoS One* 6, e26549. 10.1371/journal.pone.0026549. [PubMed: 22046307]
- Xie H, Zhang Y, Zhang P, Wang J, Wu Y, Wu X, Netoff T, and Jiang Y (2014). Functional study of NIPA2 mutations identified from the patients with childhood absence epilepsy. *PLoS One* 9, e109749. 10.1371/journal.pone.0109749. [PubMed: 25347071]
- Yi F, Danko T, Botelho SC, Patzke C, Pak C, Wernig M, and Südhof TC (2016). Autism-associated SHANK3 haploinsufficiency causes Ih channelopathy in human neurons. *Science* 352, aaf2669. 10.1126/science.aaf2669.
- Zhang Y, Pak C, Han Y, Ahlenius H, Zhang Z, Chanda S, Marro S, Patzke C, Acuna C, Covy J, et al. (2013). Rapid single-step induction of functional neurons from human pluripotent stem cells. *Neuron* 78, 785–798. 10.1016/j.neuron.2013.05.029. [PubMed: 23764284]
- Zhou LT, Ye SH, Yang HX, Zhou YT, Zhao QH, Sun WW, Gao MM, Yi YH, and Long YS (2017). A novel role of fragile X mental retardation protein in pre-mRNA alternative splicing through RNA-binding protein 14. *Neuroscience* 349, 64–75. 10.1016/j.neuroscience.2017.02.044. [PubMed: 28257890]
- Zhu PJ, Khatiwada S, Cui Y, Reineke LC, Dooling SW, Kim JJ, Li W, Walter P, and Costa-Mattioli M (2019). Activation of the ISR mediates the behavioral and neurophysiological abnormalities in Down syndrome. *Science* 366, 843–849. 10.1126/science.aaw5185. [PubMed: 31727829]

Highlights

- Analysis of hPSC models of DS and FXS
- DS and FXS hPSC models share dysregulation of synaptic and mitochondrial proteins
- DS and FXS hPSC models share transcriptional overlap, including in EIF2 signaling
- FMRP regulates DS-implicated genes in *trans*

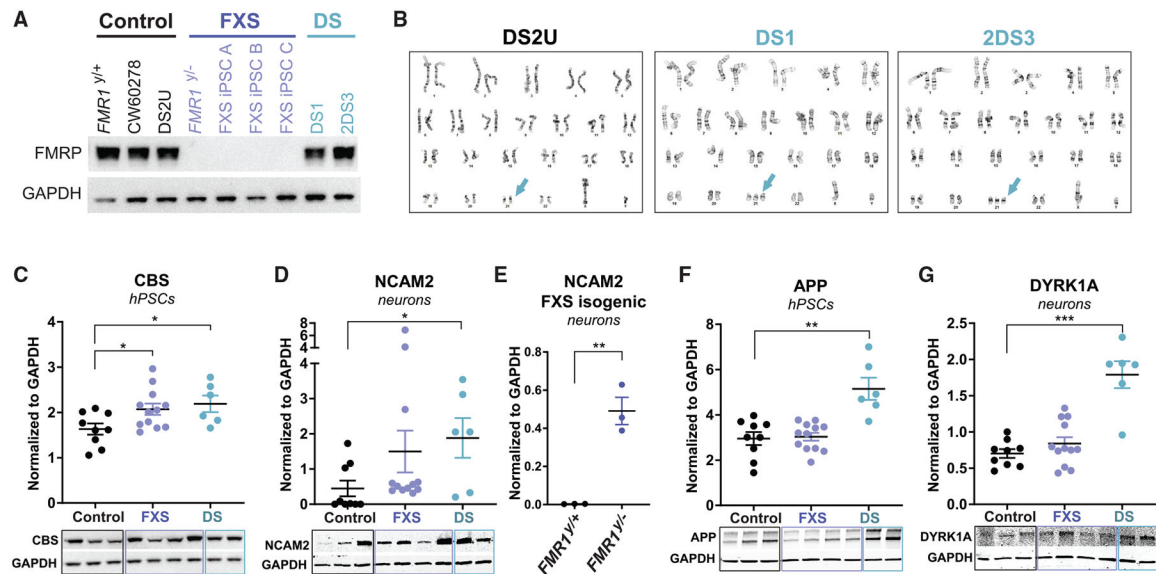


Figure 1. DS and FXS share specific protein-level perturbations in hPSC models

(A) Western blot of FMRP using *in-vitro*-derived glutamatergic neurons from the indicated cell lines confirming *FMR1* genotypes. A blot for the GAPDH loading control is shown below FMRP. As expected, neurons generated from the FXS patient iPSC lines and *FMR1*^{-/-} line lacked FMRP expression.

(B) Cytogenetic analysis of G-banded metaphase cells shows expected 46, XY karyotype for the DS2U euploid control iPSC line and 47, XY, +21 karyotypes for DS1 and 2DS3 patient iPSC lines. The blue arrow indicates HSA21.

(C and D) Quantification of western blots performed in triplicate for CBS (C) and NCAM2 (D), using the three control cell lines, four FXS cell lines, and two DS cell lines shown in (A). An example blot is shown beneath the quantification.

(E) Quantification of western blots performed in triplicate for NCAM2 using isogenic *FMR1*^{+/+} and *FMR1*^{-/-} cell lines extracted from the dataset shown in (D).

(F and G) Quantification of western blots performed in triplicate for APP (F) and DYRK1A (G) using the three control cell lines, four FXS cell lines, and two DS cell lines shown in (A). An example blot is shown beneath the quantification. For western blot quantifications, error bars show SEM and significance between control and disease samples was calculated by unpaired two-tailed t test. Significance is indicated by *p < 0.05, **p < 0.005, and ***p < 0.0005 relative to controls. See also Figure S1 and Tables S1 and S2.

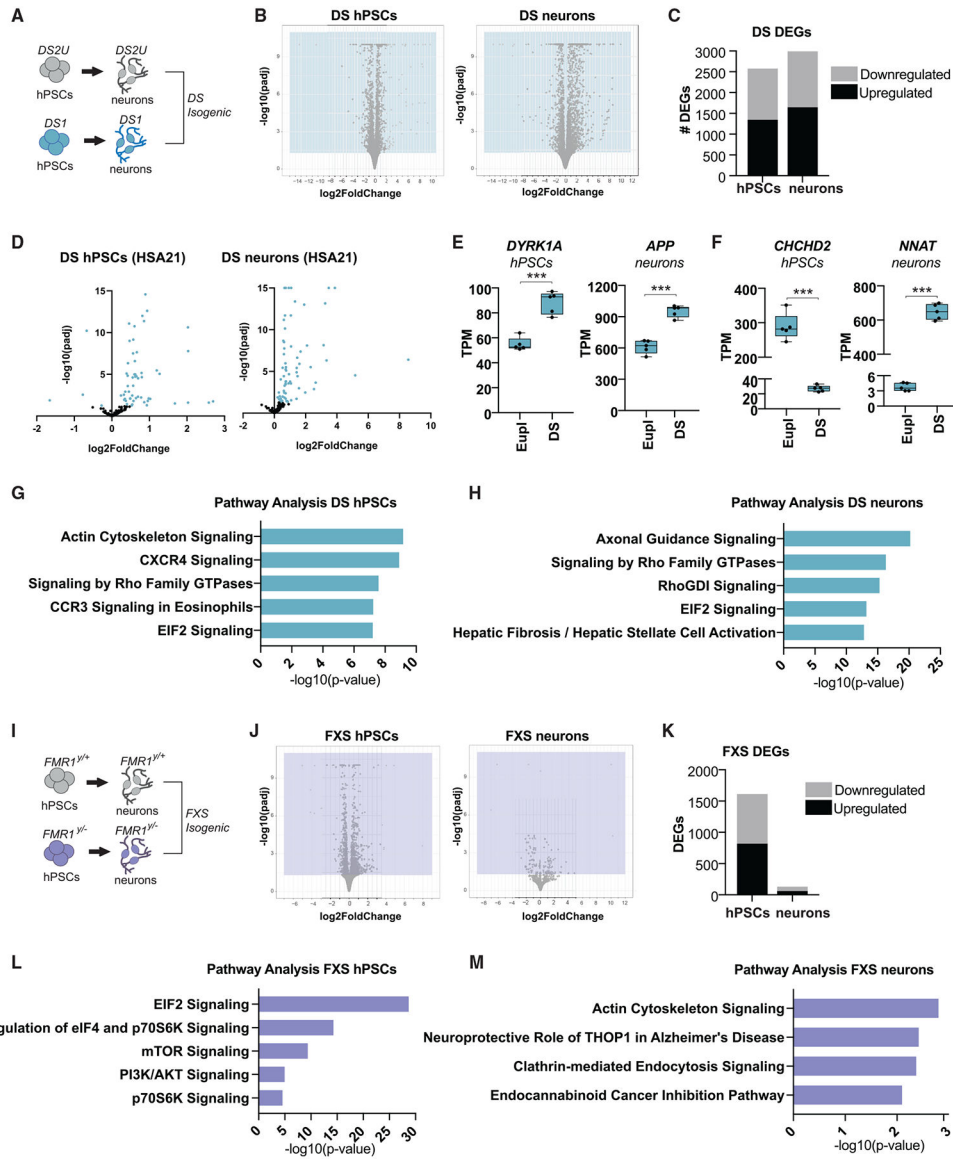


Figure 2. Mapping global transcriptional dysregulation in DS and FXS hPSC models
 (A) Schematic of isogenic DS cell lines used for RNA-seq analysis, including five replicates per cell line and genotype.
 (B) Volcano plots of transcripts from DS hPSCs (left) and neurons (right). Log₂ fold change is shown on the x axis, with the -log₁₀ of the adjusted p value shown on the y axis. Positive fold change reflects an increase in DS cells relative to euploid cells. Transcripts that reach significance of p < 0.05 are shown in the blue shaded area.
 (C) Bar chart showing the total number of significant DEGs for both DS hPSC and neuron datasets as well as the number downregulated (gray) versus upregulated (black).
 (D) Volcano plot of HSA21-encoded transcripts from hPSCs (left) and neurons (right). Log₂ fold change is shown on the x axis, with the -log₁₀ of the adjusted p value shown on the y axis for all transcripts detected from HSA21. Transcripts that reach significance of p < 0.05 are shown as blue dots.

(E and F) Examples of expression patterns for individual genes, including two encoded on HSA21 and strongly implicated in DS disease biology (E) and the two genes that were most significantly differentially expressed in the hPSC and neuron datasets (F). TPM values are shown for five replicates per condition.

(G and H) Top 5 most significant terms identified by canonical pathway analysis using IPA in the DS hPSC dataset (G) and neuron dataset (H). The $-\log_{10}(p \text{ value})$ for each term is shown on the x axis.

(I) Schematic of isogenic FXS cell lines used for RNA-seq analysis, including five replicates per cell line and genotype.

(J) Volcano plots of transcripts from FXS hPSCs (left) and neurons (right). \log_2 fold change is shown on the x axis, with the $-\log_{10}$ of the adjusted p value shown on the y axis. Positive fold change reflects an increase in *FMR1*^{-/-} cells relative to *FMR1*^{+/+} cells. Transcripts that reach significance of $p < 0.05$ are shown in the purple shaded area.

(K) Bar chart showing the total number of significant DEGs for both FXS hPSC and neuron datasets as well as the number downregulated (gray) versus upregulated (black).

(L and M) Top 5 most significant terms identified by canonical pathway analysis using IPA in the FXS hPSC dataset (L) and neuron dataset (M). The $-\log_{10}(p \text{ value})$ for each term is shown on the x axis. For all panels, significance was calculated by Benjamini-Hochberg adjusted Wald test as part of a DEseq2 RNA-seq experiment and is indicated by * $p < 0.05$, ** $p < 0.005$, and *** $p < 0.0005$ relative to control. See also Tables S3 and S4.

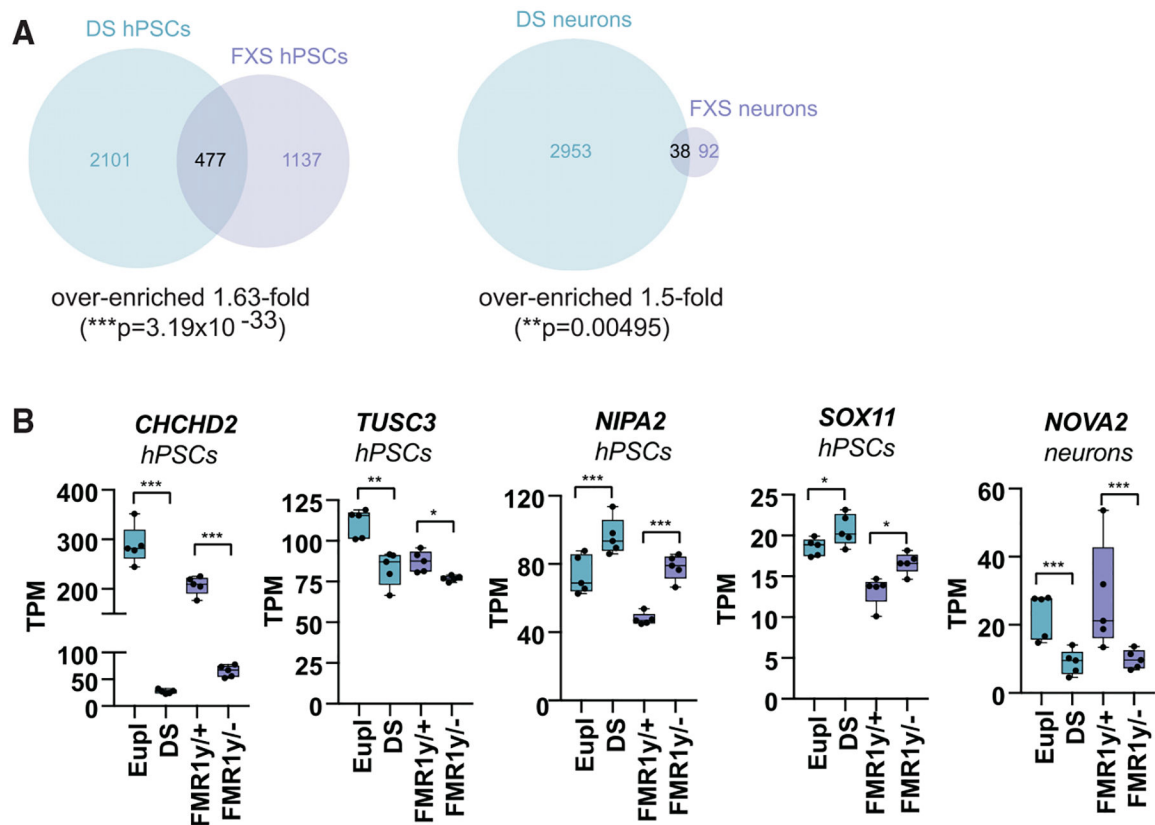


Figure 3. Transcriptional overlap between DS and FXS hPSC models

(A) Left: overlap (shown as number of genes) between DEGs identified in the DS hPSC dataset and the FXS hPSC dataset (1.63-fold over-enrichment; $p = 3.10 \times 10^{-33}$). Right: overlap (shown as number of genes) between DEGs identified in the DS neuron dataset and the FXS neuron dataset (1.5-fold over-enrichment; $p = 0.00495$). Significance was determined by hypergeometric test for over- or under-enrichment.

(B) Examples of expression patterns for individual genes with shared perturbations in FXS and DS hPSC and neuron models. TPM values are shown for five replicates per condition. Significance was calculated by Benjamini-Hochberg adjusted Wald test as part of the DESeq2 RNA-seq experiment. For all panels, significance is indicated by * $p < 0.05$, ** $p < 0.005$, and *** $p < 0.0005$ relative to the indicated control. See also Figure S2 and Tables S3 and S4.

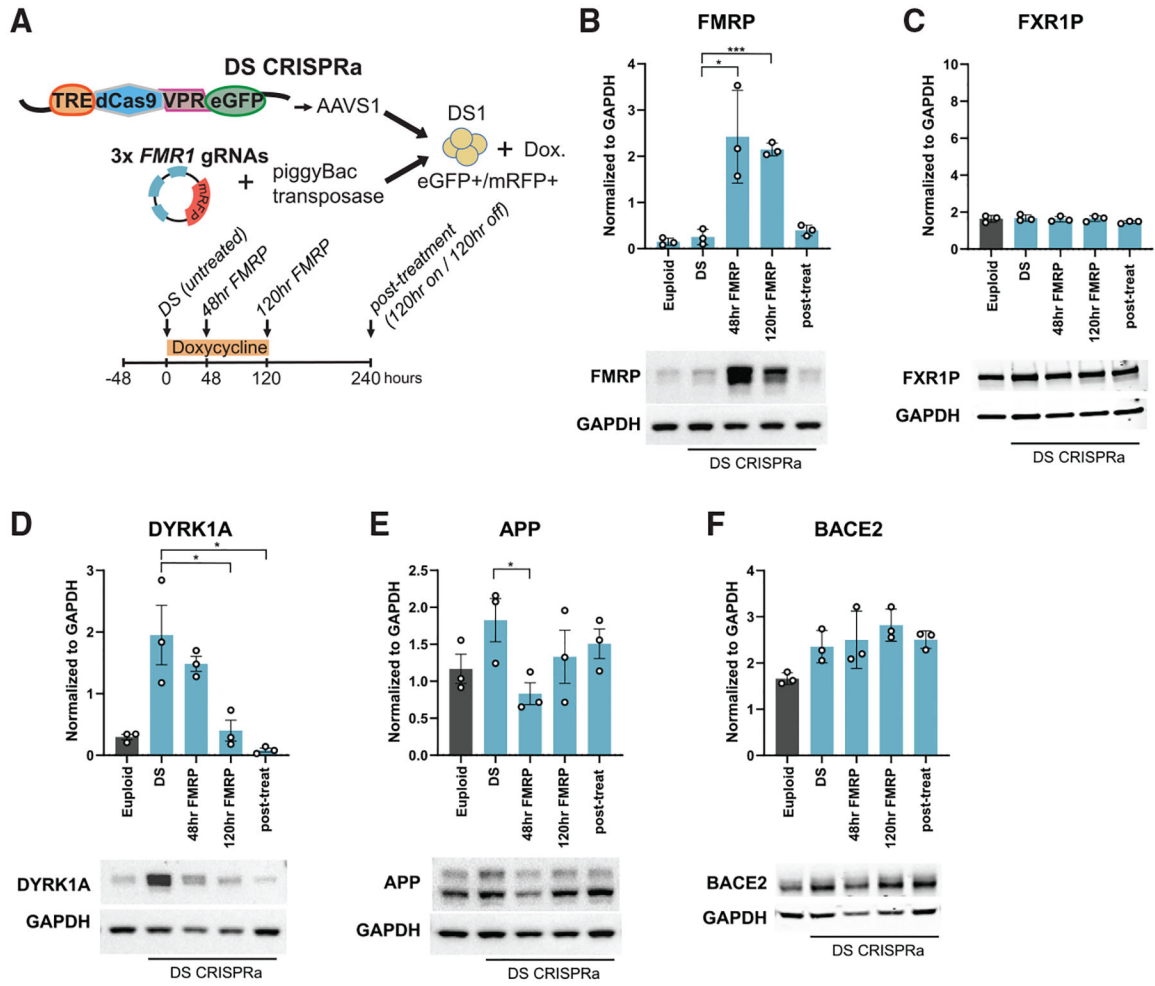


Figure 4. FMRP upregulation is sufficient to reduce expression levels of select DS-implicated proteins

(A) Schematic of DS CRISPRa experiment. Top: TRE-dCas9-VPR-eGFP was stably integrated into the AAVS1 safe-harbor locus of the DS1 cell line along with three *FMR1*-activating gRNAs introduced with a multiplexed piggyBac integration strategy. Bottom: time course of doxycycline (dox) treatment of the DS CRISPRa cell line and sample collection. (B–F) Quantification of FMRP (B), FXR1P (C), DYRK1A (D), APP (E), and BACE2 (F) protein levels from the indicated treatment conditions. The DS (untreated) condition is compared with the 48 h FMRP, 120 h FMRP, and post-treatment conditions (all DS CRISPRa cell lines) and the isogenic euploid control DS2U is used as a reference point for euploid expression levels. Note that for FMRP (B), a short exposure was used to capture the 48 and 120 h time points, which had significantly more FMRP expression compared with the euploid, DS, and post-treatment time points. Error bars show SEM and significance was calculated by unpaired two-tailed t test for each time point. All western blots were performed in triplicate. For all panels, significance is indicated by *p 0.05, **p 0.005, and ***p 0.0005 relative to controls.

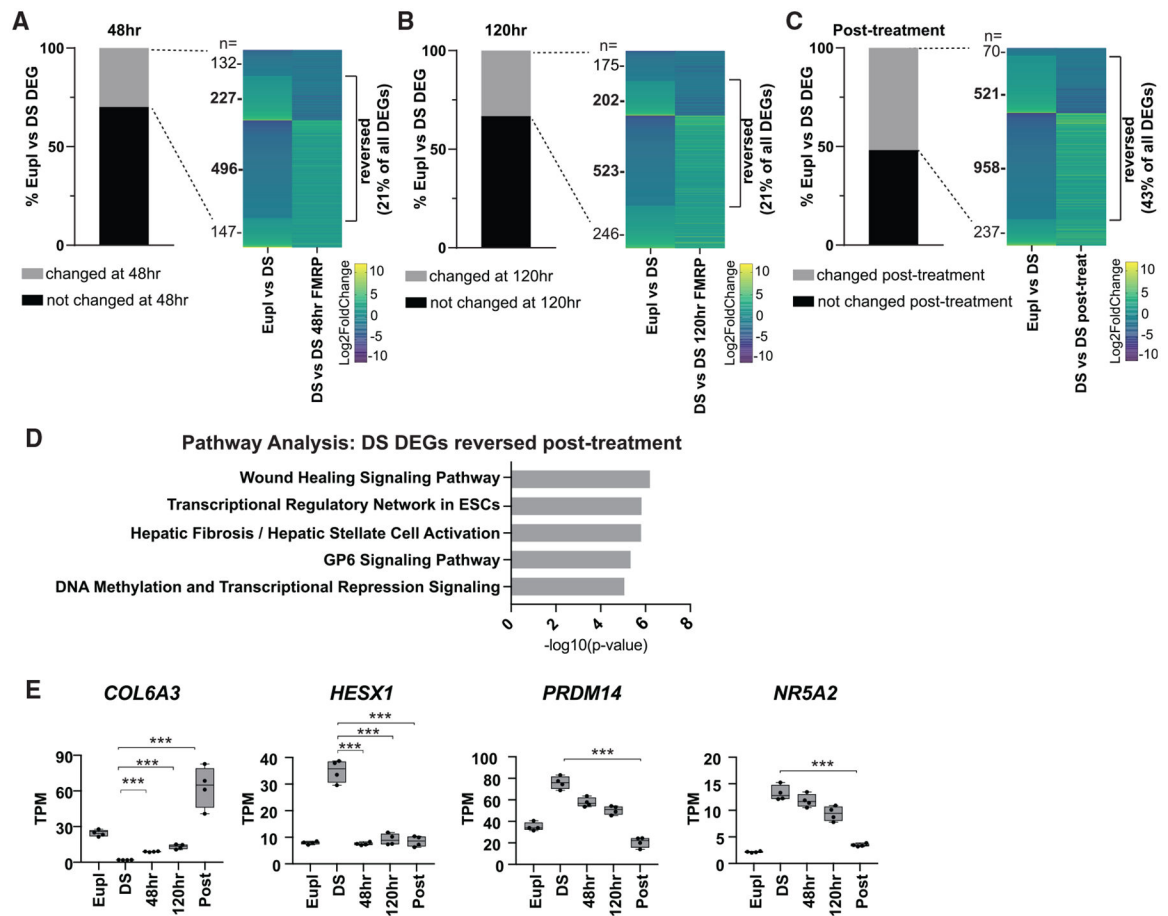


Figure 5. FMRP upregulation is sufficient to reverse over 40% of the global transcriptional perturbations in hPSC models of DS

(A–C) Left: bar graph showing 3,450 genes significantly differentially expressed between euploid and DS CRISPRa untreated cell lines. Genes that were then significantly differentially expressed following FMRP induction are shown in gray for each time point. Right: heatmaps showing \log_2 fold change for DEGs significantly changed following FMRP induction, including those that reversed directionality, at the 48 h time point (A), the 120 h time point (B), and the post-treatment time point (C). The number of genes in each category is shown to the left of each heatmap.

(D) The top 5 most significant canonical pathways (IPA) identified for DS DEGs that reversed directionality in the post-treatment time point. The $-\log_{10}(p\text{ value})$ for each term is shown on the x axis.

(E) Examples of expression patterns for individual genes across the FMRP CRISPRa time course. The DS (untreated) condition is compared with the 48 h FMRP, 120 h FMRP, and post-treatment conditions, and the isogenic euploid control is used as a reference point for euploid expression levels. TPM values are shown for four replicates per condition and significance was calculated by Benjamini-Hochberg adjusted Wald test as part of the DESeq2 RNA-seq experiments. For all panels, significance is indicated by *p < 0.05, **p < 0.005, and ***p < 0.0005 relative to controls. See also Figure S3 and Table S5.

KEY RESOURCES TABLE

REAGENT or RESOURCE	SOURCE	IDENTIFIER
Antibodies		
Rabbit Polyclonal Anti-FMRP	Abcam	Cat# ab17722; RRID: AB_2278530
Mouse Monoclonal Anti-GAPDH	EMD Millipore	Cat# MAB374; RRID: AB_2107445
Rabbit Monoclonal Anti-NCAM2	Abcam	Ab173297
Rabbit Polyclonal Anti-DYRK1A	Bethyl Laboratories	Cat# A303-802A; RRID: AB_11218191
Rabbit Anti-FXR1P	E. Khandjian	ML-13
Rabbit Polyclonal Anti-CBS	Proteintech	Cat# 14787-1-AP; RRID: AB_2070970
Rabbit Monoclonal Anti-APP	Abcam	Cat# Ab32136; RRID: AB_2289606
Rabbit Monoclonal Anti-BACE2	Abcam	Cat# Ab270458
Chemicals, peptides, and recombinant proteins		
SB431542	Tocris	1614
LDN-193189	Stemgent	04-0074
XAV939	Stemgent	04-0046
Critical commercial assays		
AllPrep DNA/RNA/miRNA Universal Kit	Qiagen	80224
Deposited data		
RNA-seq	This paper	GEO: GSE144857; Github: https://www.ncbi.nlm.nih.gov/geo/query/acc.cgi?acc=GSE144857
Experimental models: Cell lines		
Human: hESC H1 (NIH approval number NIHhESC-10-0043)	Wicell	H1
Human: UWWC1-DS1	WiCell	UWWC1-DS1
Human: UWWC1-DS2U	WiCell	UWWC1-DS2U
Human: UWWC1-2DS3	WiCell	UWWC1-2DS3
Human: CW60278	CIRM Repository	CW60278
Human: GM05131	Coriell	FXS iPSC A
Human: GM04026	Coriell	FXS iPSC B
Human: GM09497	Coriell	FXS iPSC C
Oligonucleotides		
FMR1 gRNA: GCGCTGCTGGGAACCGGCCG	This paper	G1
FMR1 gRNA: CAGGTCGCACTGCCTCGCGA	This paper	G2
FMR1 gRNA: AGACCAGACACCCCTCCCG	This paper	G3
Recombinant DNA		
TetO-Ngn2-T2A-Puro	Zhang et al., 2013	Addgene 52047
Software and algorithms		
CRISPR-ERA tool	Liu et al., 2015	http://crispr-era.stanford.edu/

REAGENT or RESOURCE	SOURCE	IDENTIFIER
RNA-seq analysis	This paper	https://github.com/hbc/Molecular-convergence-between-Down-syndrome-and-Fragile-X-syndrome-hPSCs
PRISM	GraphPad	https://doi.org/10.5281/zenodo.6974558 N/A

Author Manuscript

Author Manuscript

Author Manuscript

Author Manuscript